



Seismic wave triggering of nonvolcanic tremor, episodic tremor and slip, and earthquakes on Vancouver Island

Justin L. Rubinstein,^{1,2} Joan Gomberg,³ John E. Vidale,¹ Aaron G. Wech,¹ Honn Kao,⁴ Kenneth C. Creager,¹ and Garry Rogers⁴

Received 16 June 2008; revised 14 October 2008; accepted 20 November 2008; published 19 February 2009.

[1] We explore the physical conditions that enable triggering of nonvolcanic tremor and earthquakes by considering local seismic activity on Vancouver Island, British Columbia during and immediately after the arrival of large-amplitude seismic waves from 30 teleseismic and 17 regional or local earthquakes. We identify tremor triggered by four of the teleseismic earthquakes. The close temporal and spatial proximity of triggered tremor to ambient tremor and aseismic slip indicates that when a fault is close to or undergoing failure, it is particularly susceptible to triggering of further events. The amplitude of the triggering waves also influences the likelihood of triggering both tremor and earthquakes such that large amplitude waves triggered tremor in the absence of detectable aseismic slip or ambient tremor. Tremor and energy radiated from regional/local earthquakes share the same frequency passband so that tremor cannot be identified during these smaller, more frequent events. We confidently identify triggered local earthquakes following only one teleseism, that with the largest amplitude, and four regional or local events that generated vigorous aftershock sequences in their immediate vicinity. Earthquakes tend to be triggered in regions different from tremor and with high ambient seismicity rates. We also note an interesting possible correlation between large teleseismic events and episodic tremor and slip (ETS) episodes, whereby ETS events that are “late” and have built up more stress than normal are susceptible to triggering by the slight nudge of the shaking from a large, distant event, while ETS events that are “early” or “on time” are not.

Citation: Rubinstein, J. L., J. Gomberg, J. E. Vidale, A. G. Wech, H. Kao, K. C. Creager, and G. Rogers (2009), Seismic wave triggering of nonvolcanic tremor, episodic tremor and slip, and earthquakes on Vancouver Island, *J. Geophys. Res.*, *114*, B00A01, doi:10.1029/2008JB005875.

1. Introduction

[2] The growing number of observations of dynamically triggered tremor [Gomberg *et al.*, 2008; Miyazawa and Brodsky, 2008; Miyazawa and Mori, 2005, 2006; Miyazawa *et al.*, 2008; Peng *et al.*, 2008; Peng and Chao, 2008; Rubinstein *et al.*, 2007; A. Ghosh *et al.*, Complex nonvolcanic tremor near Parkfield triggered by the great M_w9.2 Sumatra earthquake in 2004, submitted to *Journal of Geophysical Research*, 2008; Z. Peng *et al.*, Remote triggering of tremor around the Parkfield section of the San Andreas fault, submitted to *Journal of Geophysical Research*, 2008] and earthquakes [Hill and Prejean, 2007, and references therein] indicates that these phenomena are

more common than we previously thought and likely hold clues to the processes governing fault slip and failure. The recent observations of tremor triggered by the 2002 M7.9 Denali, Alaska earthquake on Vancouver Island, British Columbia [Rubinstein *et al.*, 2007], the stable, high-quality seismic network coverage there, and extensive work on episodic tremor and slip (ETS) in the region make Vancouver Island an ideal place to test hypotheses about the relationship of triggered tremor with the driving deformations and local conditions, and with triggered earthquakes (Figure 1). Theoretical models of frictional fault slip predict both slow aseismic and rapid earthquake slip depending on the frictional properties of the fault and its environs [Liu and Rice, 2007, and references therein]. If tremor also reflects another flavor of frictional slip (e.g., such that stress drop or rupture velocities are limited to relatively low values) [Ide *et al.*, 2007], or some secondary processes perhaps driven by changing fluid pressures, then earthquakes and tremor should occur in different locations. Some studies suggest that this is true [Kao *et al.*, 2005, 2006, 2007a; Nadeau and Dolenc, 2005; Shelly *et al.*, 2006]. Another key observation relevant to understanding tremor generation comes from a study examining the

¹Department of Earth and Space Science, University of Washington, Seattle, Washington, USA.

²Now at U.S. Geological Survey, Menlo Park, California, USA.

³U.S. Geological Survey, University of Washington, Seattle, Washington, USA.

⁴Geological Survey of Canada, Sidney, British Columbia, Canada.

Table 1. Source Information for the 30 Teleseismic and 17 Local/Regional Earthquakes Studied^a

Location	Date	Origin Time	Latitude (deg)	Longitude (deg)	Depth (km)	M_w	PGV (mm/s)	Back Azimuth From PHC (deg)
<i>Teleseisms</i>								
Irian Jaya, Indonesia	17 Feb 1996	0559:30.55	-0.89	136.95	33	8.2	0.18	274
Guerrero, Mexico	25 Feb 1996	0308:15.87	15.98	-98.07	21	7.1	0.12	135
Andreanof Islands, Aleutians	10 Jun 1996	0403:35.48	51.56	-177.63	33	7.9	0.39	291
Andreanof Islands, Aleutians	10 Jun 1996	1524:56	51.48	-176.85	26	7.3	0.16	291
Santa Cruz Islands	21 Apr 1997	1202:26.43	-12.58	166.68	33	7.8	0.18	243
Kamchatka coast	5 Dec 1997	1126:54.69	54.84	162.04	33	7.8	0.38	304
Balleney Islands	25 Mar 1998	0312:25.07	-62.88	149.53	10	8.1	0.22	217
<i>Oaxaca, Mexico</i>	30 Sep 1999	1631:15.69	16.06	-96.93	60	7.5	0.40	134
Hector Mine, California	16 Oct 1999	0946:44.13	34.59	-116.27	0	7.1	0.48	149
Kodiak Island, Alaska	6 Dec 1999	2312:33.92	57.41	-154.49	66	7.0	0.11	304
<i>Volcano Islands, Japan</i>	28 Mar 2000	1100:22.51	22.34	143.73	126	7.6	0.22	284
New Ireland, Papua New Guinea	16 Nov 2000	0454:56.74	-3.98	152.17	33	8.0	0.24	260
New Britain, Papua New Guinea*	17 Nov 2000	2101:56.49	-5.50	151.78	33	7.6	0.15	259
El Salvador	13 Jan 2001	1733:32.38	13.05	-88.66	60	7.7	0.39	126
Bhuj, India	26 Jan 2001	0316:40.50	23.42	70.23	16	7.7	0.13	343
Peru coast	23 Jun 2001	2033:14.13	-16.26	-73.64	33	8.4	0.66	129
Qinghai, China	14 Nov 2001	0926:10.01	35.95	90.54	10	7.8	0.28	330
Papua New Guinea coast	8 Sep 2002	1844:23.71	-3.30	142.95	13	7.6	0.18	268
<i>Denali, Alaska*</i>	3 Nov 2002	2212:41	63.52	-147.44	4	7.9	10.07	328
Colima, Mexico	22 Jan 2003	0206:34.61	18.77	-104.10	24	7.6	0.32	141
Tokachi-Oki, Japan*	25 Sep 2003	1950:06.36	41.81	143.91	27	8.3	0.80	299
Rat Islands, Aleutians	17 Nov 2003	0643:06.80	51.15	178.65	33	7.8	0.13	292
<i>Sumatra-Andaman Islands</i>	26 Dec 2004	0058:53.45	3.30	95.98	30	9.1	1.18	311
Northern Sumatra	28 Mar 2005	1609:36.53	2.09	97.11	30	8.6	0.39	309
Northern California coast	15 Jun 2005	0250:54.19	41.29	-125.95	16	7.2	0.24	173
Pakistan	8 Oct 2005	0350:40.80	34.54	73.59	26	7.6	0.11	343
Koryakia, Russia	20 Apr 2006	2325:02.15	60.95	167.09	22	7.6	0.44	312
Tonga	3 May 2006	1526:40.29	-20.19	-174.12	55	7.9	0.15	224
Kuril Islands	15 Nov 2006	1114:13.57	46.59	153.27	10	8.3	0.40	298
East of Kuril Islands*	13 Jan 2007	0423:21.16	46.24	154.52	10	8.1	0.68	297
<i>Local/Regional Earthquakes</i>								
Offshore Northern California	24 Jul 1996	2015:44.79	41.78	-125.91	10	6.2	0.11	173
Nootka fault zone, BC*	6 Oct 1996	2013:09.18	49.05	-127.88	10	6.3	0.06	190
Northwest of Vancouver Island, BC	30 Aug 1998	1133:33	50.91	-130.66	10	6.2	0.03	277
West of Vancouver Island, BC	2 Jul 1999	1145:31.29	49.37	-129.20	10	6.4	0.03	221
Offshore Oregon	20 Jan 2000	0941:47.34	43.65	-127.26	10	6.4	0.08	179
Offshore Oregon	2 Jun 2000	1113:49.38	44.51	-130.08	10	6.5	0.05	197
West of Vancouver Island, BC	11 Jan 2001	0004:03	48.89	-129.31	10	6.0	0.10	214
West coast of Graham Island, BC	17 Feb 2001	2011:30	53.92	-133.61	20	6.3	0.09	313
Nisqually, Washington	28 Feb 2001	1854:32.83	47.15	-122.73	51	6.8	0.04	137
Nootka fracture zone, BC*	14 Sep 2001	0445:08	48.69	-128.71	10	6.0	0.06	203
West coast Moresby Island, BC	12 Oct 2001	0502:34	52.63	-132.20	20	6.3	0.09	305
Blanco fracture zone, California	16 Jan 2003	0053:15.72	44.28	-129.02	10	6.3	0.48	190
Northwest of Graham Island, BC	12 Jul 2003	2301:38	54.65	-134.47	20	6.0	0.27	316
Northwest of Graham Island, BC	28 Jun 2004	0949:47	54.80	-134.25	20	6.8	0.16	317
Nootka fault zone, BC *	19 Jul 2004	0801:49.46	49.62	-126.97	23	6.4	0.07	165
Nootka fault zone, BC *	2 Nov 2004	1002:12.82	49.28	-128.77	10	6.7	0.01	212
Offshore Northern California	17 Jun 2005	0621:42.59	40.77	-126.57	12	6.6	0.04	176

^aEarthquakes that generated tremor-triggering waves have italicized location names and those that may have triggered earthquakes have asterisks. All local/regional events are in the USA or Canada (BC = British Columbia). All teleseismic and almost all local/regional earthquake magnitudes are moment magnitudes, M_w , although a few of the later events are energy magnitudes, Me. Peak Ground Velocities (PGV) on the vertical component at PHC are noted in the eighth column and the back azimuth to the events is listed in the last column.

tremor is more probable in regions experiencing slow slip and/or tremor. We test these hypotheses by characterizing the tremor and earthquakes triggered by the 47 posited triggering earthquakes, and noting where triggering did and did not occur. We primarily use the data from the Canadian Seismic Network (CNSN) permanent stations on Vancouver Island. At the end of the study period, the CNSN maintained a network of 9 short-period stations and 10 broadband seismometers on Vancouver Island and the islands immediately adjacent to it, but the number of stations grew significantly during our study period. Our tests also make use of earthquake and tremor catalogs and GPS data

[Rogers, 2007] (Geological Survey of Canada online bulletin available at http://seismo.nrcan.gc.ca/stnsdata/nedb/bull_e.php; U.S. Geological Survey, National Earthquake Information Center available at <http://earthquake.usgs.gov/regional/neic/>; and Pacific Northwest Geodetic Array data available at <http://www.geodesy.cwu.edu/>).

2. Tectonic Setting, ETS, and Seismicity Around Vancouver Island

[7] Vancouver Island can be divided into three tectonic regimes. The Juan de Fuca plate is subducting beneath the

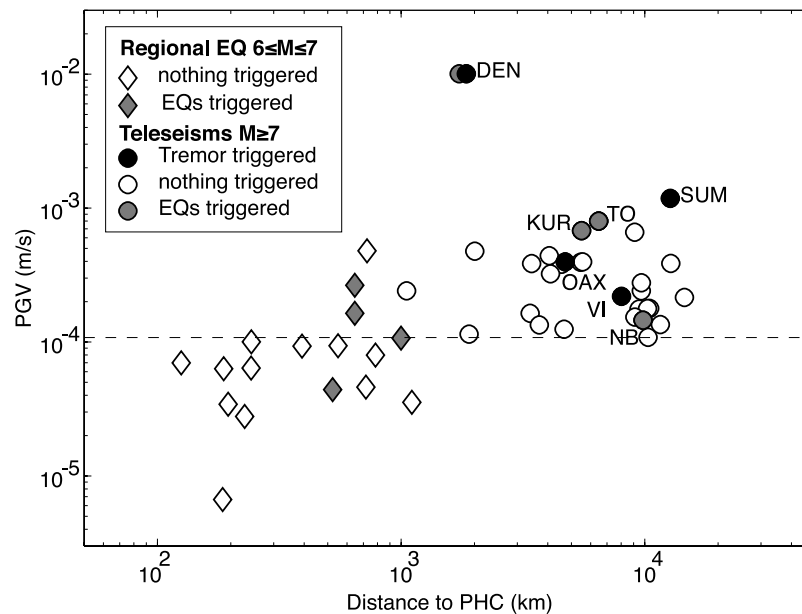


Figure 2. Peak vertical ground velocities measured at broadband station PHC plotted as a function of source station epicentral distance for the 47 earthquakes that produced the strongest shaking between 1996 and 2007. Black and gray symbols indicate earthquake waves that triggered tremor and possibly earthquakes (see text), respectively. Note that because PHC is located at the northern end of Vancouver Island (Figure 1) the distances plotted only approximate the proximity of the earthquakes to other points on Vancouver Island for shorter distances. Moreover, the peak velocities shown for the local triggering earthquakes likely underestimate the values at sites closer than PHC, possibly significantly in the near field of these events. The Denali earthquake triggered both tremor and earthquakes and is shown in black with a gray circle underlying it. We list earthquake source information in Table 1, with triggering teleseisms (circles) labeled OAX, 1999 Oaxaca, Mexico; VI, 2000 Volcano Islands, Japan; NB, 2000 New Britain, Papua New Guinea; DEN, 2002 Denali, Alaska; KUR, 2002 Kurile Islands; TO, 2003 Tokachi-Oki, Japan; SUM, 2004 Sumatra-Andaman Islands. The local/regional earthquakes (diamonds) that triggered vigorous aftershock sequences all occurred near the Nootka fault zone, and, as noted, the peak velocities likely were much larger at the triggering sites. The horizontal, dashed line marks the amplitude cutoff for the 30 largest teleseismic earthquakes.

southern half of the island and Washington and Oregon. Because of the change in orientation of the coastline at approximately the Canada-United States border, the age of the subducting plate is younger beneath Vancouver Island than to the south and the age becomes progressively younger as it approaches the northern limit of this subduction regime, which is marked offshore by the seismically active Nootka fault zone. This fault zone is a left lateral transform boundary between the Juan de Fuca and Explorer plates. North of the intersection of the Nootka fault zone with Vancouver Island the Explorer plate converges with the North America plate at less than 2 cm/a [e.g., *Braunmiller and Na'bilek*, 2002], much slower than the more rapid convergence of the Juan de Fuca Plate of about 4 cm/a. The northernmost part of Vancouver Island, north of the Brooks Peninsula, is a dramatically different tectonic regime [*Lewis et al.*, 1997]. No subducted plate can be detected beneath northernmost Vancouver Island [*Cassidy et al.*, 1998], and there appears to be no contemporary subduction.

[8] The distribution of local earthquakes in the Vancouver Island region is mostly offshore along active oceanic plate boundaries, along the outer coast where the plates begin to subduct and in the southern Strait of Georgia region extending into Puget Sound [*Ristau et al.*, 2007; *Cassidy*

et al., 2000]. Tremor tends to occur beneath Vancouver Island where local seismicity is sparse or absent [*Kao et al.*, 2005, 2006, 2007a]. The tremor source depths have been located between 10 km and 45 km beneath Vancouver Island, which would place them mostly near and above the inferred plate interface.

3. Triggered Tremor

3.1. Identification of Triggered Tremor

[9] We search for triggered tremor using all the seismic recordings from Vancouver Island for the 30 teleseismic and 17 local/regional earthquakes in the catalog described above (listed in Table 1). Each record spans 4 h, beginning at the origin time of the potential triggering event. Because the surface waves are much stronger than the tremor, we filter the seismic records to boost the tremor relative to the surface waves. We examine two partially overlapping frequency bands. We choose a 1–10 Hz bandpass filter because tremor, when not triggered, is typically strongest in this range [e.g., *Nadeau and Dolenc*, 2005; *Obara*, 2002; *Rogers and Dragert*, 2003]. We also use a 5 Hz high-pass filter because triggered tremor is stronger than ambient tremor and therefore has a particularly high signal-to-noise

ratio for these frequencies [Peng et al., 2008; Rubinstein et al., 2007].

[10] We identify triggered tremor visually, manually searching for consecutive bursts of high-frequency energy that appears to turn on and off with a periodicity similar to that of the teleseismic surface waves (Figure 3b). This is a feature common to all previous observations of triggered

tremor [Gomberg et al., 2008; Miyazawa and Brodsky, 2008; Miyazawa and Mori, 2005, 2006; Miyazawa et al., 2008; Peng et al., 2008; Peng and Chao, 2008; Rubinstein et al., 2007; Ghosh et al., submitted manuscript, 2008; Peng et al., submitted manuscript, 2008]. To minimize spurious identifications we require consecutive bursts at a minimum of two nearby stations. We identify 4 teleseismic earth-

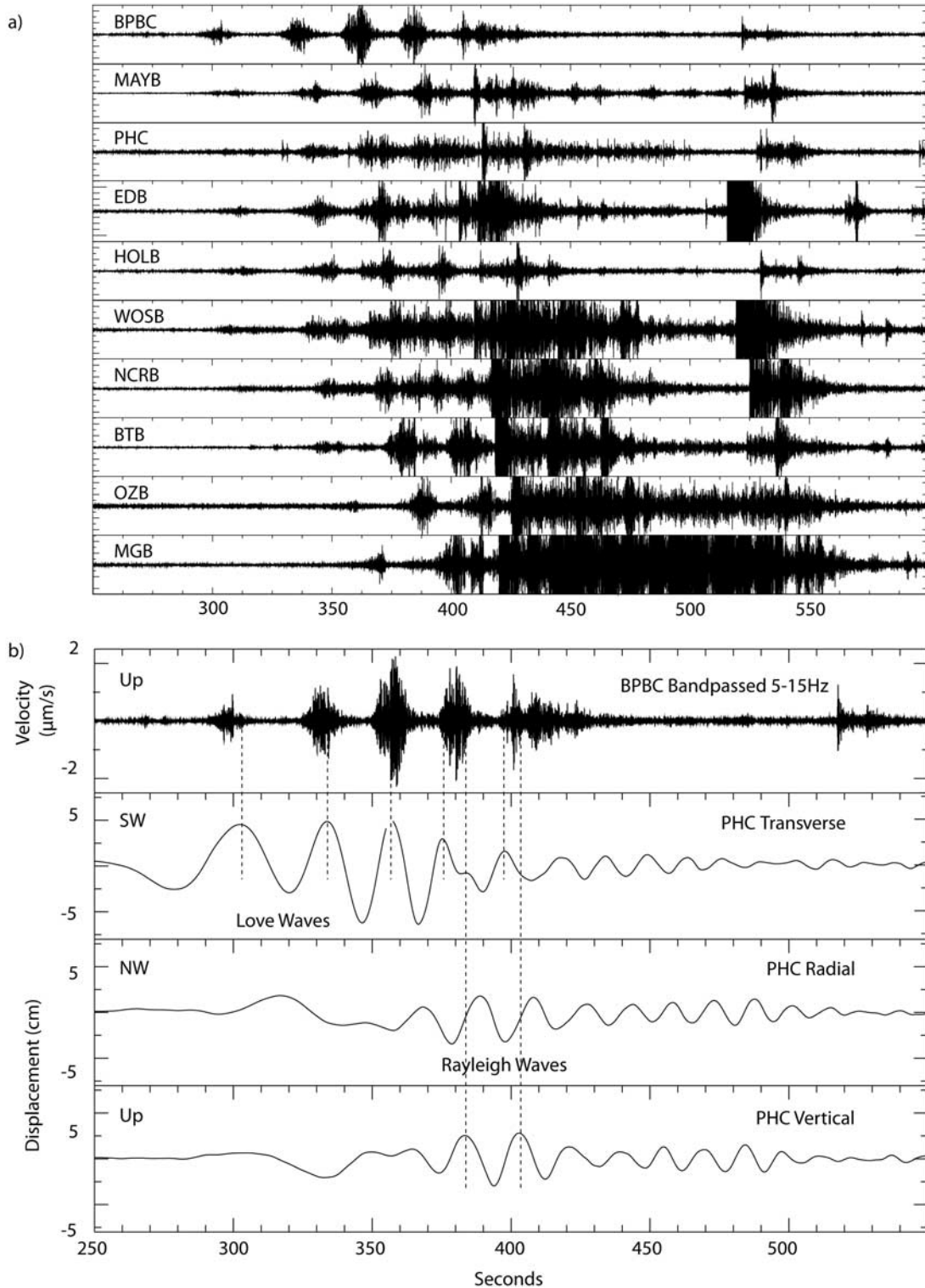


Figure 3

quakes that triggered tremor somewhere on Vancouver Island, including the 2002 Denali earthquake that was previously identified by *Rubinstein et al.* [2007] (Table 2). We note that while we searched all the data available for each event, we never identify tremor being triggered in multiple locations by a single earthquake, unlike what was observed in California for the Denali earthquake [*Gomberg et al.*, 2008]. This suggests that the probability of triggering tremor is highly dependent on local conditions, which are temporally variable. The triggered tremors are located using the same waveform envelope cross correlation method as from *Rubinstein et al.* [2007], which was based on the method of *Obara* [2002]. Each instance of triggered tremor is discussed below and the locations are listed in Table 2. The parameters of the events that triggered tremor are italicized in Table 1.

[11] We also consider the possibility that these triggering earthquakes may trigger weaker, long-lasting tremor, like that seen during an ETS event (*Ghosh et al.*, submitted manuscript, 2008; *Peng et al.*, submitted manuscript, 2008). This sort of triggering would be indicated by a sustained increase in the amount of high-frequency energy that starts with or shortly after the arrival of the surface waves from the triggering event. No such triggering was identified.

3.2. Triggered Tremor Versus Ambient Tremor

[12] In this manuscript, we routinely will refer to “ambient tremor”. By ambient tremor, we are simply referring to tremor that is not triggered by teleseismic waves (i.e., does not appear modulated by the waves of distant earthquakes). This ranges from a short burst of tremor for which no concurrent slow slip was observed to the tremor that occurs during a multiweek ETS episode where significant slip was observed by GPS instrumentation. Fundamentally, we believe these to be the same phenomenon.

[13] There is mounting evidence that triggered and ambient tremor are the same phenomenon driven by different loading deformations. Triggered tremor appears in the time domain as a series of a few seconds long bursts that rise and fall slowly and pulse with the periodicity of the causative surface waves (Figure 3), in contrast to the more irregular chatter of ambient tremor that maintains sustained amplitudes for tens of seconds to hours. Close examination of the frequency content of triggered tremors in both Cascadia [*Rubinstein et al.*, 2007] and California [*Peng et al.*, 2008] show that while triggered tremor is sometimes up to ten times larger in amplitude than ETS and ambient tremor, they share a common 1–30 Hz spectral slope that is

Table 2. Parameters of Triggered Tremor^a

Triggering Earthquake	Latitude (km)	Longitude (km)	Computed Depth ^b (km)	Depth to Interface ^c (km)
Denali	50.19 ± 6	−127.61 ± 4	19	15
Sumatra	50.08 ± 20	−127.45 ± 20	5	15
Oaxaca	48.80 ± 10	−124.3 ± 5	18	40
Volcano Islands	49.65 ± 10	−125.9 ± 5	15	35

^aLocations of triggered tremors identified in this study. Locations are determined using the same waveform envelope cross-correlation method as *Rubinstein et al.* [2007].

^bUncertainties for the depths computed with this method are not included as they are very high (>20 km).

^cThe depth to the interface at the epicentral location is also noted, as this is the depth we assume the triggered tremor is occurring at. This depth is used in computing S arrival times for the tremor (i.e., Figures 3b, 4b, 5b, and 6b).

significantly different from earthquakes. The common spectral slope suggests that both flavors of tremor arise from the same physical process.

[14] Polarization analysis of tremor supports this inference. Tremor triggered by the Sumatra earthquake in Japan appeared to be dominated by S waves with polarizations perpendicular to the strike of the subduction zone [*Miyazawa and Brodsky*, 2008]. Ambient tremor in Cascadia is also dominated by S waves polarized in the direction of relative plate motion [*Wech and Creager*, 2007]. These findings and focal mechanism studies of many slow slip phenomena in Japan [*Ide et al.*, 2007] all suggest that tremor, regardless of whether it’s ambient or triggered tremor, reflects shear slip on the plate interface with the same sense of slip as that expected from plate motions.

3.3. Tremor Triggered by Teleseismic Earthquakes

[15] The association of triggered tremor with Rayleigh or Love waves provides constraints on the physical mechanisms that cause it [*Miyazawa and Brodsky*, 2008; *Miyazawa and Mori*, 2006; *Rubinstein et al.*, 2007]. There is evidence that tremor triggered by both Love and Rayleigh waves is an instantaneous frictional response to a change in the local stress state on the plate interface, such that tremor turns on when the waves increase the Coulomb stress, and turns off when Coulomb stress is reduced.

[16] For the case of the 2002 Denali earthquake, *Rubinstein et al.* [2007] showed that Love waves traveling parallel to the trench offshore Vancouver Island turn tremor on when displacements are in the direction of plate motion related slip on the interface (SW), and off when in the direction

Figure 3. (a) From *Rubinstein et al.* [2007, Figure S1]. Section of 10 vertical-component seismograms arranged by distance from the triggered tremor, showing clear moveout of the tremor. Traces have been filtered between 5 and 15 Hz and scaled to make the tremor easily identifiable. The additional impulsive bursts of energy at 420 and 520 s are triggered earthquakes in a different location than the tremor. Time is relative to 2216 UTC. (b) Modified from *Rubinstein et al.* [2007, Figure 3]. Comparison of tremor and the surface waves that triggered it, “corrected” so both correspond to the tremor source location. (top seismogram) Tremor recorded on the vertical component of the closest station BPBC, time-adjusted by 5.14 s to reflect the travel time of S waves from the tremor source to BPBC. (bottom three seismograms) Instrument-corrected displacement seismograms for the transverse, radial, and vertical components at PHC, the closest three-component, broadband station to the tremor, shifted by 8.40 s to reflect the difference in arrival time of the third and largest Love wave pulse at PHC and at the tremor source. Vertical, dashed lines represent the time of peak shear (for Love waves) and peak dilatation (for Rayleigh waves) for the surface waves, and thus representing the time we expect triggered tremor to be at its peak.

opposite of the direction of slip (NE). They note that the stresses correlate with displacement because the Love wave displacement amplitudes are decreasing with depth, creating a displacement gradient (i.e., a strain) across the relatively flat plate interface. Therefore, to analyze the relationship between stress from the Love waves and the triggered tremor we rotate displacement seismograms of the surface waves such that they are in a trench-parallel and trench-perpendicular orientation. On the basis of their work on the Denali earthquake, *Rubinstein et al.* [2007] argue that triggered tremor represents a frictional failure response to changing stress conditions on the plate interface.

[17] Rayleigh waves have been shown to trigger tremor, with several studies using the in-phase relationship between tremor occurrence and upward vertical surface displacements to infer that tremor occurs when the dilatation is positive [*Miyazawa and Brodsky*, 2008; *Miyazawa and Mori*, 2006]. As shown in Appendix A, the vertical displacements should be indicative of dilatational strains or stresses at depth, although the correctness of the positivity inference is guaranteed only assuming a homogeneous, isotropic, half-space Earth model. *Miyazawa and Mori* [2006] and *Miyazawa and Brodsky* [2008] suggest two models for triggered tremor: frictional failure and permeability pumping. Pumping involves oscillatory fluid flow that is modulated by changing permeability levels that are responding to changes in dilatation and normal stress, which in turn changes the Coulomb failure stresses.

3.3.1. The 2002 Denali Earthquake

[18] The shaking from the Denali earthquake was the strongest to hit Vancouver Island in the 11-year study period, producing peak ground velocities nearly an order of magnitude greater than the next largest, which came from the Sumatra earthquake (Figure 2). Even though the Denali earthquake shaking was much stronger than any of the other events considered, we only identify 5 bursts of tremor over the course of 150 s, coming from near the Brooks Peninsula (Figure 1). The tremor was observed at stations over 250 km away from its source (Figure 3a). The seismic records from Southern Vancouver Island suggest that there may have been tremor triggered there also, but the tremor was obscured by strong, local, triggered earthquake activity.

[19] To determine the causative relationship between the Love waves from the Denali earthquake and the triggered tremor we take the closest recordings of the surface waves and the tremor to the tremor source and shift them in time such that they reflect their timing at the tremor source [*Rubinstein et al.*, 2007]. The epicentral location of the

triggered tremor source is accurate, but the depth is poorly constrained. We assume the tremor is radiating from the plate interface at 15 km depth and fix the hypocenter of the tremor at this depth. This analysis shows that shear stresses associated with the Denali Love waves strongly control the presence of tremor, while the weaker Rayleigh waves do not (Figure 3b) [*Rubinstein et al.*, 2007].

3.3.2. The 2004 Sumatra Earthquake

[20] The shaking from the Sumatra event was the second strongest to hit Vancouver Island in the 11-year study period. Like the Denali event, tremor was triggered near the Brooks Peninsula (Figure 1). This tremor was observed at stations up to ~ 150 km away from the tremor. This suggests that the tremor triggered by the Sumatra earthquake was weaker than that triggered by the Denali earthquake, which was observed over 250 km from the tremor source. We infer that the tremor triggered by the Sumatra earthquake is weaker because the driving stress is smaller. Although the Sumatra earthquake's peak amplitudes were much smaller than those from Denali, the surface waves from Sumatra persist much longer than those radiated by the Denali earthquake. The relative durations of the Sumatra and Denali wave trains, ~ 2000 and 250 s, respectively, are consistent with the longer-lasting triggered tremor for the Sumatra earthquake (approximately 50 bursts instead of 5; Figure 4a).

[21] We investigate the timing relationship of the surface waves and the tremor, assuming the tremor is on the plate interface (15 km) because the depth is poorly constrained (Figure 4b). Tremor occurs during the arrival of both the Love and Rayleigh waves. The observations do not appear consistent with the aforementioned theoretical predictions that the tremor should correspond to displacements to the SW for the Love waves and upward for the Rayleigh waves. This plausibly may be attributed to the very large uncertainty in the epicenter of the Sumatra-triggered tremors (>20 km), which translates into arrival time differences of 4–5 s, or the possibility of multiple source regions (see Figure 4).

3.3.3. The 1999 Oaxaca Earthquake

[22] The 1999 $M_w 7.4$ Oaxaca, Mexico earthquake also triggered tremor on Vancouver Island. Relative to many other teleseismic earthquakes during our study period, the peak broadband velocity was not particularly strong (Figure 2) and was, in fact, markedly smaller than that from the Denali and Sumatra events. An ETS event was ongoing in Southern Vancouver Island at the time of the Oaxaca earthquake and it may have facilitated the triggering of tremor. The Oaxaca-triggered tremor pulsed approximately

Figure 4. Same as Figure 3 but for the 2004 Sumatra earthquake waves. Note the much longer duration of tremor relative to that from the Denali surface waves (Figure 3). Time is relative to 0058 UTC. (a) Section of five vertical seismograms arranged by distance from the triggered tremor. Traces have been high-pass filtered at 3 Hz and scaled to make the tremor easily identifiable. While the moveout of individual bursts suggests that there may be several sources, application of the location procedure which is based on maximizing envelope correlations, shows that multiple locations are not resolvable. (b) Comparison of tremor and the surface waves that triggered it, corrected so both correspond to the tremor source location. (top seismogram) Tremor recorded at the closest station BPBC, time-adjusted by 8.01 s to reflect the travel time of S waves from the tremor source to BPBC. (bottom three seismograms) Instrument-corrected displacement seismograms for the dip-parallel, strike-parallel, and vertical components at EDB, the closest three-component, broadband station to the tremor, shifted by 8.33 s, the difference in arrival time of the largest Rayleigh wave pulse at EDB and at the tremor source. Vertical, dashed lines represent the time of peak shear (for Love waves) and peak dilatation (for Rayleigh waves) for the surface waves, and thus representing the time we expect triggered tremor to be at its peak.

20 times and was seen at stations more than 100 km away from the source (Figure 5a).

[23] Tremor from the Oaxaca earthquake begins during the strong shaking of the Love waves and continues as the Rayleigh waves pass by the site (Figure 5b). As with the previous events, the depth of the tremor triggered by the Oaxaca earthquake is poorly constrained so we set the depth

of the tremors to be at 40 km, the approximate depth of the plate interface. The tremor triggered by the Love waves is consistent with the frictional model suggested by *Rubinstein et al.* [2007], in that the tremor turns on when displacements are to the southwest, amplifying the regional stress field and turns off when displacements are to the NE, resisting slip on the plate interface. The vertical Rayleigh wave displacements

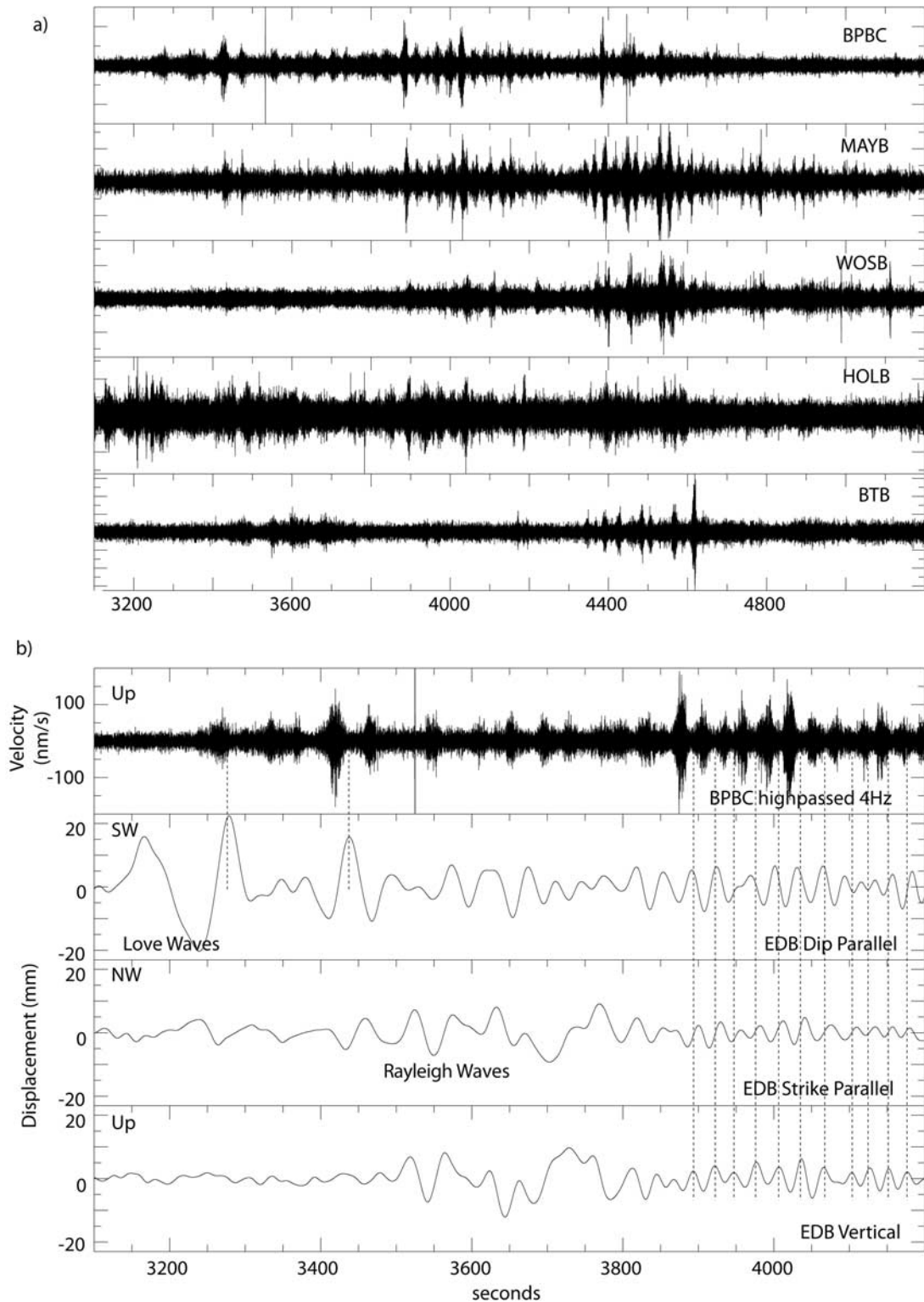


Figure 4

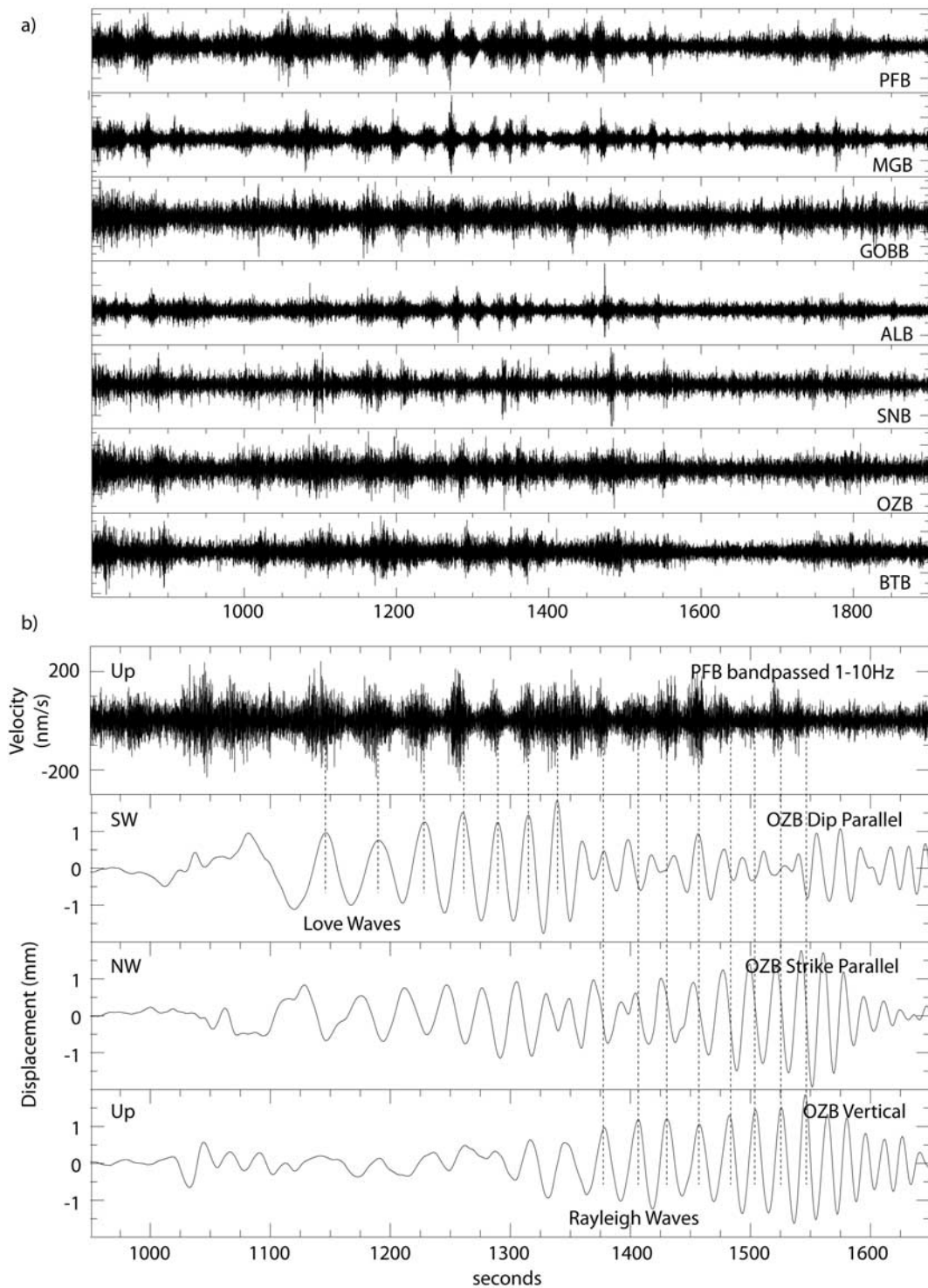


Figure 5. Same as Figure 3 but for the 1999 Oaxaca earthquake waves. Time is relative to 1631 UTC. (a) Section of seven vertical seismograms arranged by distance from the triggered tremor. Traces have been filtered between 1 and 10 Hz and scaled to make the tremor easily identifiable. (b) Comparison of tremor and the surface waves that triggered it, corrected so both correspond to the tremor source location. (top seismogram) Tremor recorded at the closest station PFB, time-adjusted by 12.73 s to reflect the travel time of S waves from the tremor source to PFB. (bottom three seismograms) Instrument-corrected displacement seismograms for the dip-parallel, strike-parallel, and vertical components at OZB, the closest three-component, broadband station to the tremor, shifted by 17.43 s, the difference in arrival time of the largest Love wave pulse at OZB and at the tremor source. Vertical, dashed lines represent the time of peak shear (for Love waves) and peak dilatation (for Rayleigh waves) for the surface waves, and thus representing the time we expect triggered tremor to be at its peak.

also correspond nicely to the tremor, implying that dilatation from the Rayleigh waves also modulates the strength of the triggered tremor.

3.3.4. The 2000 Volcano Islands Earthquake

[24] The 2000 $M_w7.6$ Volcano Islands, Japan earthquake is the fourth earthquake we observed to trigger tremor on Vancouver Island. Of these four events, this earthquake shook Vancouver Island (Figure 2) with the smallest peak velocities. Tremor triggered by this earthquake was observed to a similar distance range (>100 km) (Figure 6a) as the tremor triggered by the Sumatra and Oaxaca earthquakes. Tremor became clearly observable during the arrival of the Rayleigh waves and weaker tremor may have also been triggered by the Love waves (Figure 6b). The timing of the tremor relative to both the Love and the Rayleigh waves is that the tremor is consistently early relative to the surface waves. If our expectations of tremor being an immediate response to both shear and dilatational loading are correct, then this would suggest that a location error has caused the disagreement in timing as this disagreement is consistent throughout the tremor wave train. It is also noteworthy that waves from other earthquakes with larger peak velocities than those for both this earthquake and the triggering Oaxaca event failed to trigger tremor. We discuss the implications of the in section 5.

3.4. Tremor Triggering by Regional and Local Earthquakes

[25] The results of our search for tremor triggered by regional and local earthquakes are inconclusive. This is not necessarily because the tremor was weak or nonexistent but rather because it cannot be separated from the posited triggering waves. This leaves open the possibility that triggered tremor may occur commonly in association with more frequent smaller earthquakes, but is inherently difficult to observe. We carefully examined all 17 events in our catalog, but we were not able to identify any tremor triggered by these earthquakes because, in the frequency band of the tremor, the energy from the earthquakes themselves is stronger (Figure 7). For example, waves in the tremor passband radiating from an $M_w6.3$ earthquake located near Graham Island and recorded ~ 750 km to the southeast at short-period station BTB has peak amplitudes of $\sim 20,000$ counts. The largest triggered tremor amplitude we observe for any teleseism at any station is over an order of magnitude smaller (associated with the Denali earthquake at BPBC with tremor peak amplitude of approximately 1,200 counts) and tremor amplitudes associated with the smaller teleseisms are typically on the order of 200 counts. The peak broadband amplitudes of the triggering teleseismic waves are of comparable or greater size than those of this regional event (Figure 2). Thus, we conclude that if tremor is triggered by these events, it will be hidden in the much louder roar of the high-frequency body waves and coda from these regional and local events.

4. Tremor Triggering and the Importance of Driving Deformation Characteristics

[26] The probability of earthquake waves triggering tremor likely depends on both the characteristics of the waves and the conditions at the site of posited triggering. In this

section we focus on the influence of driving deformation on the probability of tremor triggering. In the following subsections we examine a number of aspects of the surface waves that may influence whether tremor is triggered.

4.1. Amplitude

[27] The two events with the strongest shaking on Vancouver Island in the 11-year span of our study (the 2002 $M_w7.9$ Denali and 2004 $M9.1$ Sumatra earthquakes) both triggered tremor. We also identify tremor triggered by the $M_w7.4$ Oaxaca and $M_w7.6$ Volcano Islands earthquakes. The peak velocities from these earthquakes are significantly smaller than many earthquakes for which we did not observe any triggered tremor (Figure 2). A similar pattern is seen when we examine peak displacement or peak acceleration, in that Sumatra and Denali had the largest deformations of all the earthquakes, but the Oaxaca and Volcano Islands earthquakes had deformations that were neither particularly large nor small. Given these findings, we argue that amplitude contributes, but alone does not appear to be a sufficient criterion to trigger tremor except in cases of the two very largest deformations. This differs from the triggered tremor in Parkfield, California, which appears at the time of the strongest peak velocities (Peng et al., submitted manuscript, 2008). Our finding also contrasts with previous studies that argue that the amplitude of tremor may scale with amplitude of stressing [Miyazawa and Brodsky, 2008; Rubinstein et al., 2007]. We note that except for the tremor triggered by the Denali earthquake, there does not appear to be a connection between the amplitude of the individual surface wave pulses on Vancouver Island and the amplitude of the tremor bursts. The amplitudes of all the triggered tremors on Vancouver Island, except those triggered by Denali, are very similar despite the fact that the driving displacements are highly variable from earthquake to earthquake, ranging from ~ 0.5 mm to ~ 20 mm. All of these observations indicate that amplitude, while it is likely important in determining whether an earthquake will trigger tremor, it is not the only condition controlling whether tremor will be triggered at Vancouver Island. We speculate below on why tremor is triggered by the very largest dynamic deformations and only some of the smaller ones.

4.2. Frequency

[28] Our observations permit us to make a few conclusions about the dependence of tremor triggering on the frequency of the triggering waves. First, they suggest that lower frequencies (hundreds of seconds period or more) are not required to trigger tremor. Because of the Sumatra earthquake's extraordinary size, the waves it radiated undoubtedly contained energy at lower frequencies not present in the much smaller, tremor-triggering Oaxaca and Volcano Island earthquakes. Unfortunately we cannot conclude anything about if and how the tremor triggering passband might be limited at the high-frequency end. The triggered tremor correlates temporally with the arrival of the surface waves, which are the largest amplitude waves. The largest amplitude waves of all four tremor-triggering earthquakes have periods in the 20–100 s range, and the energy outside this passband diminishes rapidly. This band-limited excitation and the difficulty separating tremor from the higher-frequency waves of the local and regional posited

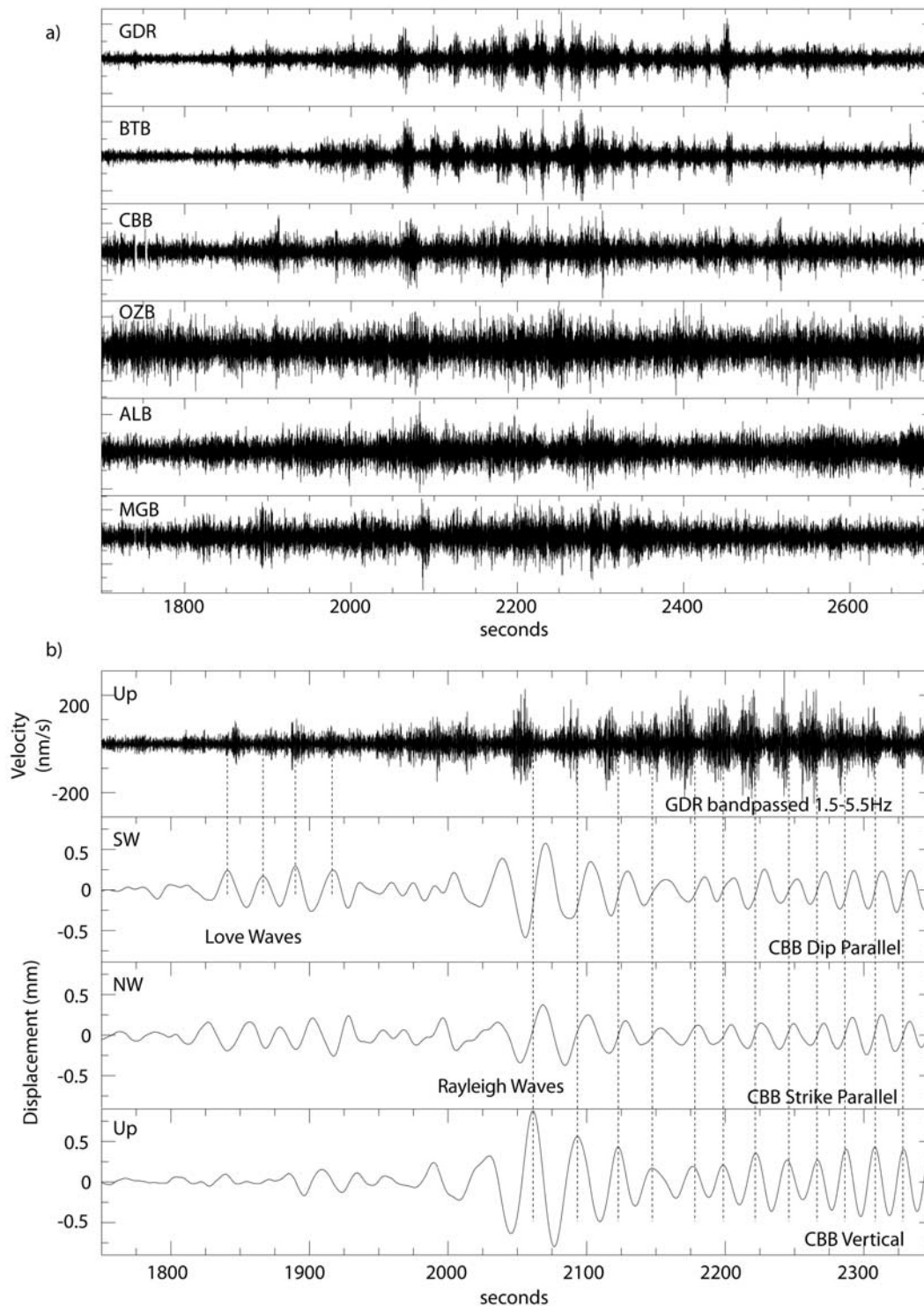


Figure 6. Same as Figure 3 but for the 2000 Volcano Islands earthquake waves. Time is relative to 1100 UTC. (a) Section of six vertical seismograms arranged by distance from the triggered tremor. Traces have been filtered between 1.5 and 5.5 Hz and scaled to make the tremor easily identifiable. (b) Comparison of tremor and the surface waves that triggered it, corrected so both correspond to the tremor source location. (top seismogram) Tremor recorded at the closest station GDR, time-adjusted by 10.33 s to reflect the travel time of S waves from the tremor source to GDR. (bottom three seismograms) Instrument-corrected displacement seismograms for the dip-parallel, strike-parallel, and vertical components at CBB, the closest three-component, broadband station to the tremor, shifted by 10.13 s difference in arrival time of the largest Love wave pulse at CBB and at the tremor. Vertical, dashed lines represent the time of peak shear (for Love waves) and peak dilatation (for Rayleigh waves) for the surface waves, and thus representing the time we expect triggered tremor to be at its peak.

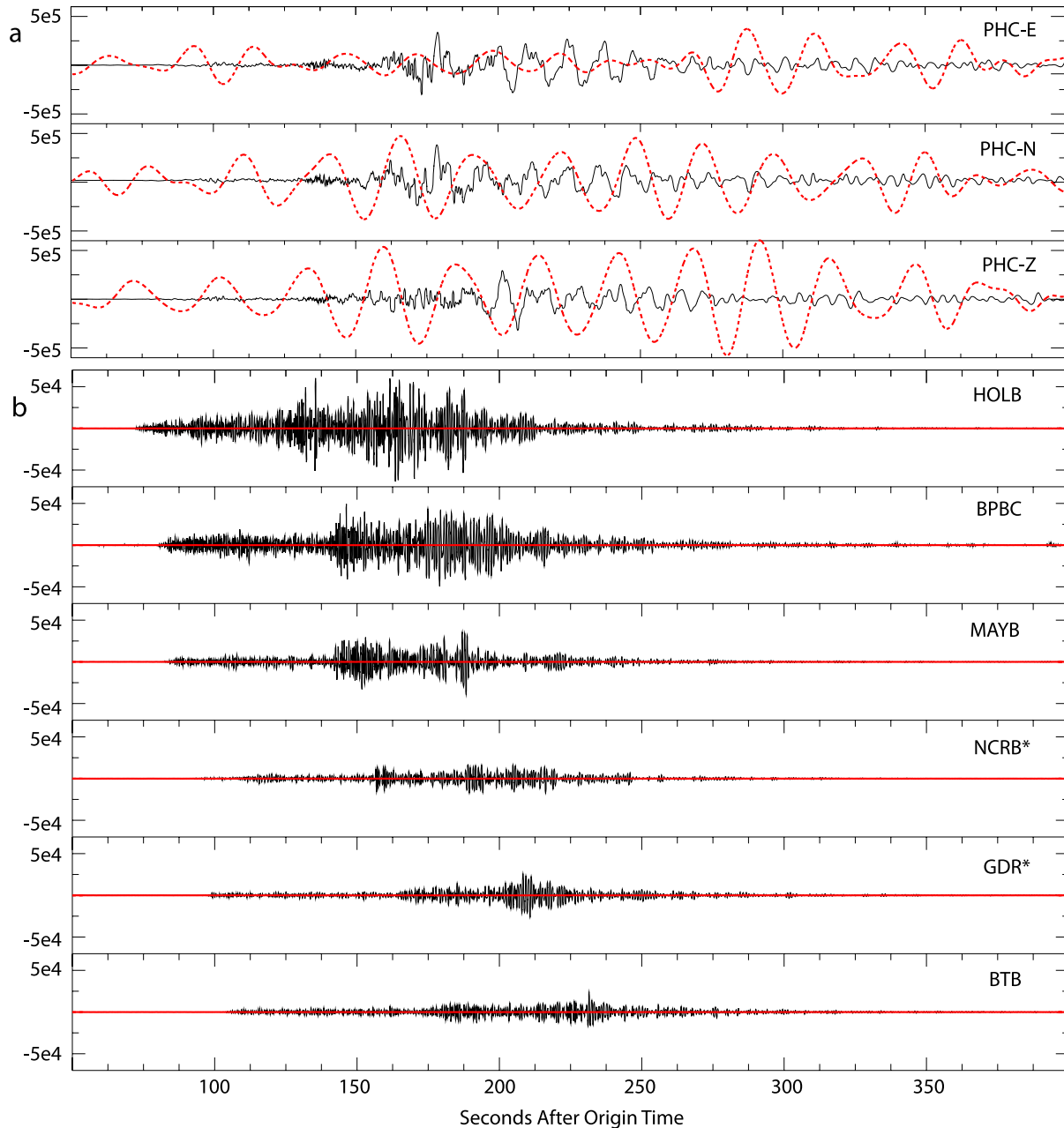


Figure 7. (a) Broadband velocity seismograms for an M_w 6.3 regional earthquake located northwest of Vancouver Island (solid) and the Sumatra earthquake (dashed), both recorded at station PHC. (b) Seismograms of the M_w 6.3 earthquake filtered to emphasize energy in the tremor passband (between 5 and 15 Hz) recorded at stations ordered by increasing distance from the source (solid). The moveout and duration indicate that this energy originates at the M_w 6.3 earthquake source. The seismograms of the Sumatra earthquake waves filtered in this same passband are plotted on top of the recordings of the regional earthquake (thin horizontal lines centered within recordings of the regional earthquake). Note that even though Sumatra-generated tremor would be visible with an expanded vertical scale, if tremor triggered by a regional earthquake had similar amplitudes as those triggered by the Sumatra event it would be subsumed by the energy from the regional earthquake. For the recordings of the regional event, the horizontal scale represents the number of seconds after the earthquake origin time. For the recordings of the Sumatra earthquake, the time origin is arbitrary; all the data from Sumatra are from more than 1 h after the origin time. Stations that are starred are stations where tremor triggered by the Sumatra earthquake was not observed.

triggering events limits what can be inferred above the passband of the surface waves from these smaller triggering teleseisms.

4.3. Azimuth: Love Waves Versus Rayleigh Waves

[29] As noted above, the timing of triggered tremor relative to the arrival of Love or Rayleigh waves generally does not rule out either as causative and thus does not permit definitive conclusions about the triggering efficacy of shear, normal, or dilatational stresses. This is because the Love waves and Rayleigh waves often arrive simultaneously. In the case of the Denali, Sumatra, and Oaxaca earthquakes (Figures 3, 4, and 5) the Love waves clearly triggered tremor but the tremor continues on after the arrival of the Rayleigh waves. For example, for the Sumatra event, a significant amount of tremor occurs when the Rayleigh waves are largest and the Love waves have diminished in amplitude significantly, and for the Volcano Islands earthquake there is very weak, if any tremor triggered by the Love waves.

[30] This leads us to examine the polarization as a possible discriminant. If triggering of tremor reflects an enhancement of shear stressing parallel to the convergence direction of the subducting and overriding plates as argued by *Rubinstein et al.* [2007], then we might expect triggering waves to be more commonly polarized such that Love or S waves propagate parallel to the plate margin (assuming the tremor source is on the plate margin). Dilatational deformations, arising exclusively from Rayleigh waves, are isotropic and thus the orientation of the fault they act upon does not matter. However, the relative contribution of shear to dilatational deformations, or equivalently Love to Rayleigh waves, depends on how the radiation pattern is sampled and thus the orientation of the fault plane and slip that radiate, and the azimuth from the source to the fault acted upon. Unfortunately, we lack sufficient diversity of earthquake back azimuths to search for such variations.

5. Tremor Triggering and the Importance of Local Conditions

[31] We now consider the importance of the characteristics of the affected fault and its surroundings on its potential to be triggered as tremor. Frictional models and explanations of tremor and slow slip require specific environmental conditions and thus, if applicable to triggered tremor, would predict its occurrence in specific regions. For example, ambient tremor beneath Vancouver Island has been located between 25 and 45 km depth [*Kao et al.*, 2005, 2006, 2007a], consistent with temperature and dehydration regimes [*Peacock et al.*, 2002] needed for frictional models that predict slow, episodic slip [*Liu and Rice*, 2007]. The epicenters of the tremor sources triggered by the Oaxaca and Volcano Island earthquake waves locate above the 40 km depth contour defining the plate interface [*McCrorry et al.*, 2003]. While their depths are uncertain they are consistent with frictional or fluid-related models. However, the Denali and Sumatra tremor sources locate where the plate interface is considerably shallower, suggesting that higher temperatures and pressures and perhaps fluids may facilitate tremor triggering but are not requirements. That said, we note that this shallower triggered

tremor is likely on or above the plate interface between the North American and the Explorer plates, which has much younger, and therefore warmer, subducting crust than the interface between the North American and Juan de Fuca plates.

[32] We test the hypothesis that slow slip facilitates triggering by examining the coincidence of when and where triggering occurred, when teleseisms failed to trigger, and when and where slow slip occurred as inferred from GPS data and tremor activity. To make this comparison, we use the Cascadia-wide catalog of GPS observations of ETS episodes from *Szeliga et al.* [2008] and a catalog of tremor that spans the last 25 years for the Southern Vancouver Island/Northern Puget Sound ETS region [*Rogers*, 2007]. For those events where we don't have tremor records that clearly indicate an end to the ETS episode, we assume the slip events last two weeks on the basis of an average duration of slow slip events during ETS episodes in Cascadia.

[33] Of the 30 teleseismic earthquakes examined, only one clearly occurred during an ETS event; this was the 1999 Oaxaca earthquake, one of the four that we have identified as having triggered tremor. The Oaxaca earthquake occurred during the tail end of the 1999 ETS event and the tremor source its waves triggered is located in the middle of the region that was actively radiating tremor at the time (Figure 8). This suggests that the ongoing slow slip in the region facilitated the triggering of tremor. However, the connection directly to slow slip is conjectural, based on the apparent connection between slow slip and tremor during ETS events [*Szeliga et al.*, 2008]. One could also argue that the tremor rate, at the time of the triggering is particularly high, thus indicating a relatively larger fraction of the region is close to failure (as tremor) making the triggering of tremor more likely. This would be analogous to earthquake triggering, which is more common in regions of high ambient seismicity.

[34] Our observations also indicate that ongoing slow slip or high rates of ambient or ETS tremor do not guarantee that tremor will be triggered if a teleseism shakes the region vigorously. In addition to the tremor triggered by the Oaxaca earthquake, we also examine the tremor triggered by the Volcano Islands earthquake. The tremor triggered by the Volcano Islands earthquake occurred during a quiet time of no detected tremor or slow slip. A few bursts of tremor occurred 2 days prior to the Volcano Islands earthquake, and curiously it and the triggered tremor sources locate in approximately the same place. However, such isolated short-lived bursts are common and precede nontriggering earthquakes by similar intervals.

[35] We also conclude that ongoing or recent tremor or slow slip is not a necessary condition for triggering tremor as the tremor triggered by 2002 Denali earthquake occurred in the demonstrable absence of tremor and slow slip in the region. The tremor triggered by the 2004 Sumatra event also appears to have occurred in the absence of slow slip and tremor. This assertion is equivocal as there is a GPS station that indicates there may have been ongoing slow slip, but a systematic study of tremor in the region does not identify any ongoing tremor at the time [*Kao et al.*, 2007a]. The locations of the tremor sources that were triggered by the Sumatra and Denali earthquake waves corroborate this conclusion. They locate slightly north (<25 km) of most

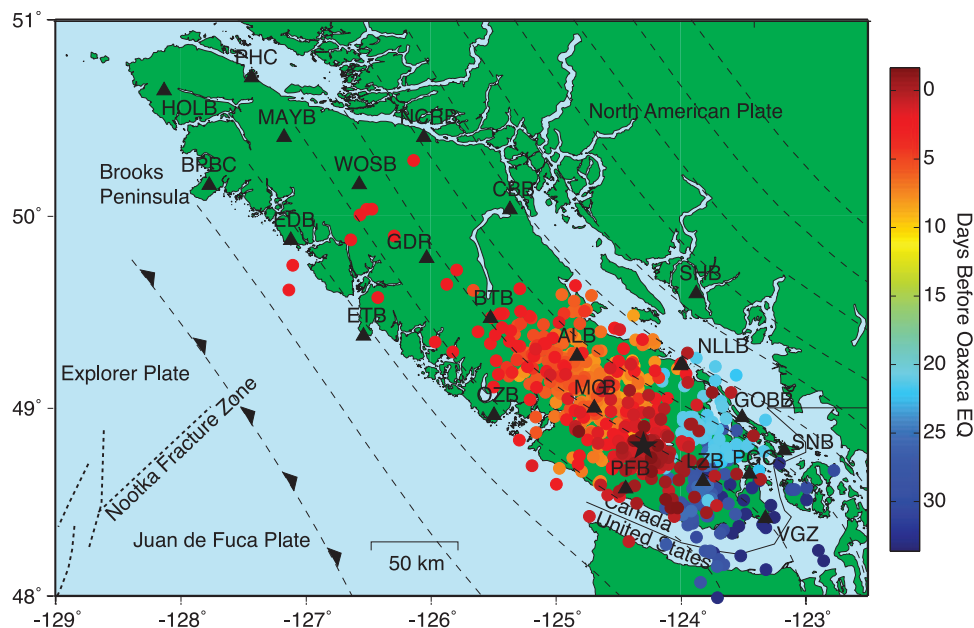


Figure 8. Tremor sources (colored circles) during the 1999 episodic tremor and slip (ETS) episode in southern Vancouver Island located using the method of *Kao et al.* [2007b]. Circles are such that their color reflects their timing relative to the Oaxaca earthquake. The Oaxaca earthquake occurred on 30 September, near the end of the ETS event. The GPS data also indicate that slow slip was underway in this same area. The tremor sources migrate with time, and the triggered tremor source (star) occurs in the same location as most of the tremor at the time of the triggering earthquake. If the migration of slow slip (not resolvable in the GPS data) follows the location of tremor, this suggests the slow slip facilitated the triggering.

ambient tremor [*Kao et al.*, 2007a] beneath the Brooks Peninsula (Figure 1). These observations of triggering by relatively large waves are easier to explain than that for the relatively very small Volcano Island earthquake waves. Intuitively and as frictional and other failure models would predict, a sufficiently large perturbing deformation could render the initial conditions on the fault nearly irrelevant and bring it to failure. We have no explanation for the Volcano Islands triggering.

6. Triggered Earthquakes

[36] We examined all available seismograms from stations on Vancouver Island for signals from locally generated earthquakes during the 4 h after the origin time of each posited triggering earthquake. To enhance local earthquake signals relative to those of the posited triggering events, we high-pass-filtered (corner 5 Hz) these seismograms and picked P and S wave arrival times manually (e.g., see Figure 9). We located local earthquakes using a grid search algorithm [*Gomberg et al.*, 1990] that permits

hypocenters to be estimated with only a few phases, although in such cases the uncertainties are large. Most of the local earthquakes occurred offshore, limiting location accuracy to as much as tens of km in the worst cases; however, this is not problematic for the inferences we wish to make. For reasons noted below, we considered a rate increase potentially significant if more than four to six local/regional earthquakes were detected in the 4 h examined. For the posited teleseismic triggering earthquakes, we find the only unambiguous seismicity rate increase followed the 2002 M_w 7.9 Denali earthquake (Figure 10), and questionable increases for the 2007 M_w 8.1 Kuriles, 2003 M_w 8.3 Tokachi-Oki, and 2000 M_w 7.8 New Britain earthquakes.

[37] For the posited regional and local $M \geq 6.0$ triggering earthquakes we find no locatable triggered earthquakes within the study area (48° – 51° N, 123° – 129° W) in the subsequent 4 h, with the exception of the four $M \geq 6.0$ earthquakes on the Nootka fault zone (Figure 1). These Nootka fault zone earthquakes generated numerous aftershocks in the vicinity of the fault zone. Although we did not locate these aftershocks, we verified that they all had

Figure 9. High-pass-filtered (corner 5 Hz) vertical component velocity seismograms (top nine traces in Figures 9a and 9b) from Vancouver Island stations showing signals from the first nine local earthquakes to occur within the wave train of the Denali earthquake (broadband trace at station PHC at the bottom of Figures 9a and 9b). Horizontal components are shown for stations PFB and LZB because of low signal-to-noise on the verticals, and, in general, S wave arrivals were picked from horizontal components. P and S wave arrival times were picked manually and used to locate each earthquake (Figure 10) are labeled, with numbers referring to the epicentral information in Table 3. Dashed box indicates when tremor was triggered: triggered tremor can be seen in a number of the seismic records.

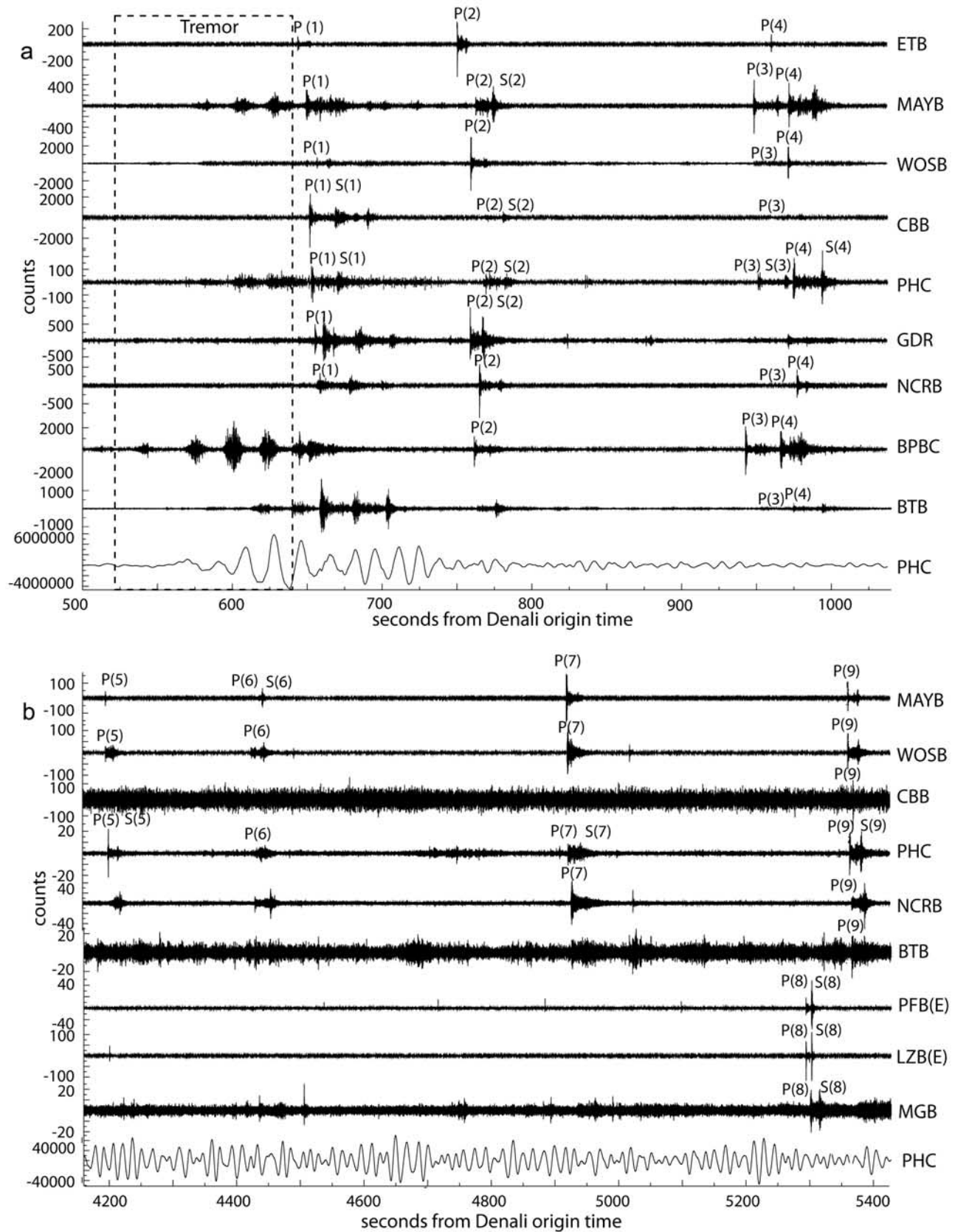


Figure 9

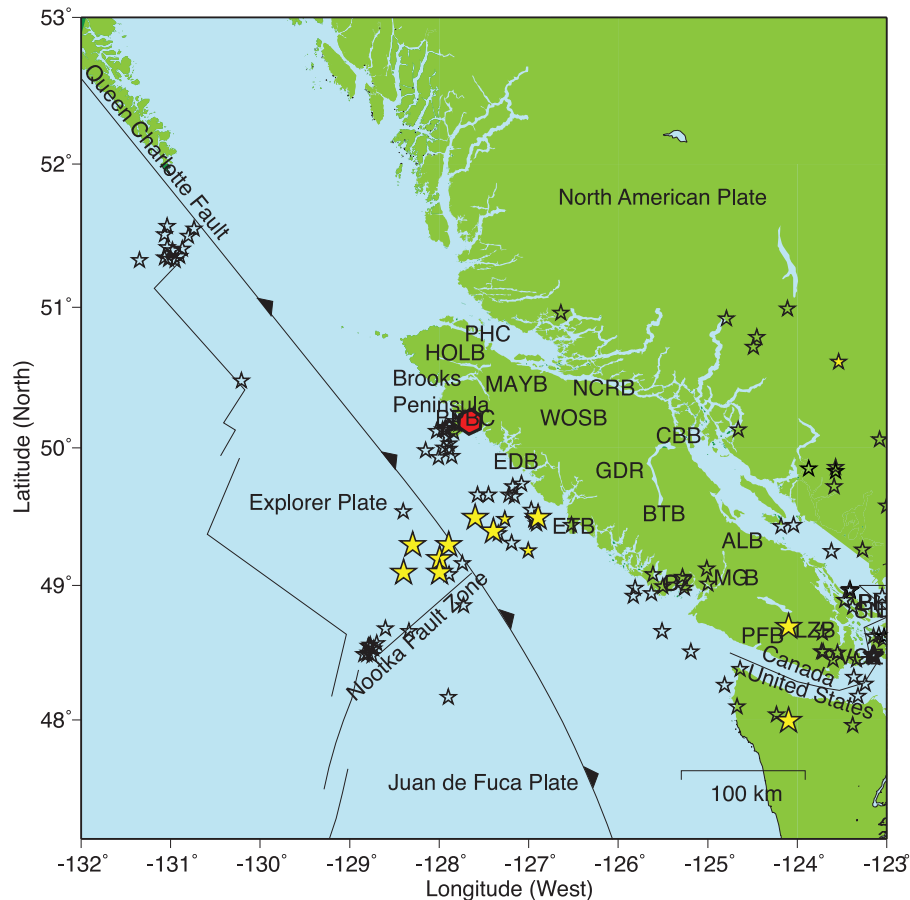


Figure 10. Epicenters of earthquakes that occurred within 4 h after the Denali earthquake in (small filled stars) and not in (large filled stars) the Geological Survey of Canada catalog, and cataloged during the 2 months preceding the Denali earthquake (small open stars). The hexagon shows the location of the tremor source triggered by the Denali earthquake waves. Locations of seismic stations are indicated by the corresponding station code.

approximately the same arrival time move out as the corresponding main shock, suggesting no significant triggering occurred far from the main shock. However, applying the same criteria as for the teleseismic posited triggering events, the aftershocks of the posited triggering $M \geq 6.0$ Nootka fault zone earthquakes should be considered triggered activity, i.e., following each event the seismicity rates clearly increased within the study area.

[38] We identify triggering as an increase in the seismicity rate relative to the ambient rate, concurrent with and immediately following the causative deformation, as in many other studies. We assess the probability that an increased rate observed during the 4 h starting with the origin time of the posited triggering earthquake is significant by comparing it to that expected owing to random chance (i.e., ambient seismicity). We use the Geological Survey of Canada (GSC) catalog spanning 1 year prior to the earthquake to estimate the ambient rate. However, we interpret these catalog-based probabilities conservatively, noting they likely underestimate those appropriate to our analyses because they do not account for the fact that earthquakes cluster temporally and spatially, and we have attempted to identify and locate all possible earthquakes and in some cases using only a few, barely visible, phases.

Nonetheless, we estimate a catalog-based probability that the rate observed in a 4-h time window reflects a random process by counting the number of earthquakes in 1000 randomly selected 4-h windows and calculate histograms of these counts. These indicate an approximately 73% chance that no earthquakes will be observed, a 20% chance of observing a single earthquake, less than 0.5% of observing four events, and almost no chance of seeing six or more earthquakes. To assess probable magnitudes for events not cataloged, we measure and plot the RMS amplitude of the P waves at each station, noting also the corresponding magnitude for cataloged earthquakes.

[39] Only the rate increase following the 2002 $M_w 7.9$ Denali earthquake is unambiguous, even given ambiguities in several of the local/regional earthquakes identified. Within 4 h after the Denali origin time we identify and locate 13 local/regional earthquakes (see Figures 9 and 10 and Table 3) and note that a few others could be identified but were not located. The first ten are not in the GSC catalog and the first two have amplitudes significantly larger than those of the cataloged events. Most occur within the Nootka fault zone (Figure 10) and several may be aftershocks of the initial events based on their spatial proximity, but even discounting these leaves an earthquake rate diffi-

Table 3. Denali-Triggered Earthquakes^a

Event	Date	Time	Latitude (N)	Longitude (W)	Magnitude
1	3 Nov 2002	22:22:43*	49.4	-127.4	
2	3 Nov 2002	22:24:30*	49.5	-126.9	
3	3 Nov 2002	22:27:42*	49.2	-128.0	
4	3 Nov 2002	22:27:59*	49.1	-128.0	
5	3 Nov 2002	23:21:55*	49.5	-127.6	
6	3 Nov 2002	23:25:29*	49.1	-128.4	
7	3 Nov 2002	23:34:00*	49.3	-128.3	
8	3 Nov 2002	23:40:14*	48.0	-124.1	
9	3 Nov 2002	23:41:21*	49.3	-127.9	
10	3 Nov 2002	23:58:08	50.62	-123.54	1.3
11	4 Nov 2002	00:08:12	49.26	-127.01	1.1
12	4 Nov 2002	00:26:06	49.49	-127.27	0.9
13	4 Nov 2002	00:43:05*	48.7	-124.1	

^aCatalog of local earthquakes within the first 4 h following the 2002 M7.9 Denali, Alaska earthquake. Times with asterisks are for those events we identify and are absent from the GSC catalog and correspond to the arrival time of the earliest arriving P wave because our location algorithm does not solve for origin time. GSC catalog origin times, epicenters and magnitudes are entries without asterisks.

cult to attribute to random chance. None of the earthquakes during this 4-h period locate near the tremor triggered by the Denali waves (Figure 10), or any of the tremor triggered by other earthquakes (Figure 1).

[40] We note three other teleseisms that were followed by four to six local earthquakes within 4 h, but for the reasons cited above and below, we interpret these only as suggestive of a triggered rate increase. We identified six local/regional events in the 4 h following the 2007 M_w 8.1 Kuriles earthquake; four of these are in the GSC catalog with magnitudes ≤ 2.4 . The epicenter of one event is possibly within kilometers of the tremor source triggered by the Denali earthquake, and all occur in areas of relatively high ambient seismicity rates. Five local events can be identified following the 2003 M_w 8.3 Tokachi-Oki earthquake; the third earthquake and largest, a M3.5 event, was reported in the GSC catalog. For two others only P wave arrivals can be measured at only three stations. The fifth event is close enough to the first to be considered triggered by it instead of the teleseismic waves. Two of these earthquakes occur along the generally active Nootka fault zone, the others occur in areas with almost no seismicity in the preceding year, and all are more than 50 km from any of the tremor locations. Five local events were identified following the 2000 M_w 7.8 New Britain earthquake. The first two are found in the GSC catalog, have magnitudes 0.5 and 1.6 and locate in areas of relatively high ambient seismicity, and the subsequent three events appear to be of the same size or smaller with arrival times just barely measurable.

7. Earthquake Triggering and the Importance of Driving Deformation Characteristics and Local Conditions

[41] The most extraordinary characteristic of the only earthquake waves that unambiguously triggered seismicity, relative to those from the other teleseisms studied, were the large amplitudes. The peak velocity measured for the Denali surface waves exceeds that of all other teleseisms by an order of magnitude. The Denali source radiated enormous Love waves (relative to the Rayleigh waves and for an

earthquake of its magnitude), focused directly at Vancouver Island implying that shear deformations triggered the seismicity rate increase. A number of studies have postulated that frequency content also affects the earthquake triggering efficacy of dynamic deformations [Gomberg *et al.*, 1997; Beeler and Lockner, 2003; Voisin *et al.*, 2004; Brodsky and Prejean, 2005; Gomberg and Johnson, 2005; Johnson and Jia, 2005; Savage and Marone, 2007]. The triggering of earthquakes by Denali waves but not by those from the Sumatra earthquake suggests that waves with frequencies below ~ 0.01 Hz are not effective earthquake triggers. We make no inferences based on amplitudes or frequency content of the local or regional earthquakes, because our amplitude measurements at PHC underestimate those experienced at the much closer distances corresponding to the vigorous aftershock sequences of the $M > 6.0$ earthquakes on the Nootka fault zone. Thus, we cannot distinguish which may be more important in triggering aftershocks, the higher frequencies of the waves (relative to the teleseismic pass-band) or larger near-field amplitudes.

[42] If local conditions (e.g., fault geometry, frictional properties, low effective stresses) are favorable for ambient seismicity one might expect it in the same places as triggered seismicity. Most of the Denali-triggered local earthquakes locate in the vicinity of the normally seismically active Nootka fault zone, although we locate a few in areas of sparse seismicity dispersed from the Olympic Peninsula to the mainland of British Columbia (Figure 9). The aforementioned other three cases of possible triggering by teleseismic waves, also are generally consistent with this expectation. For example, all six of the local earthquakes that occur within 4 h of the 2007 Kuriles earthquake locate within areas of relatively high ambient seismicity rates, although interestingly, widely dispersed geographically and in tectonic setting. Slow slip does not appear to facilitate earthquake triggering (by simple Coulomb stress transfer or some other means) since there was no significant change in the seismicity rate following the Oaxaca earthquake, the only earthquake that demonstrably occurred during an ETS episode on Vancouver Island.

8. Triggering of Episodic Tremor and Slip

[43] We now consider the possibility that teleseismic earthquakes may trigger ETS events. The first suggestion of this comes from the Southern Vancouver Island/Puget Sound ETS region. Using the criteria that the start of an ETS episode is marked by sustained tremor activity lasting 5–24 h/day [Kao *et al.*, 2006, 2007b], we note that the M_w 8.1 Kuriles earthquake on 13 January 2007 likely preceded the start of the 2007 ETS event. We verified this by examining seismic data from Washington and Southern Vancouver Island prior to the Kuriles earthquake. There was elevated tremor activity in Washington during the week preceding the Kuriles earthquake, but only 1 day had more than ~ 1 h of tremor. Additionally, by the time of the Kuriles earthquake, tremor rates had died down to a background level, ~ 20 min of tremor in 24 h.

[44] Acknowledging the possibility that the timing of the 2007 ETS episode and the Kuriles earthquake may be simply a coincidence, we further explore the relationship between the arrival of large amplitude, teleseismic surface

waves and ETS in the area by comparing the ETS catalog of *Rogers* [2007] to our catalog of 30 large teleseisms. When available (2003–2007), we supplemented the aforementioned catalog of ETS with information from the PNSN as ETS episodes in this region could start in either Washington or Southern Vancouver Island. When we compare for each ETS episode the time since the previous episode and the time since the last arrival of large teleseismic waves, we identify a remarkable feature (Figure 11). All the ETS episodes that are “late” (i.e., have recurrence times significantly longer than the average) begin shortly after a large teleseismic earthquake. There is a delay (measurable in days) between the arrival of the surface waves from these teleseismic events and the onset of the ETS. We suggest that this delay is real as it cannot be attributed to detection issues or the events starting outside of the seismic networks we are using. The delay between the teleseismic events and the onset of the ETS is variable for these potentially triggering earthquakes, ranging from 0 to 15 days. It is unclear as to what kind of process could trigger ETS and have a highly variable delay between excitation and onset of ETS. A similar observation has been made in Japan, whereby periods of tremor appear to be triggered by nearby medium magnitude events [*Obara*, 2002]. One interpretation is that for these late slip events the plate interface is on the verge of failure, such that the small perturbations associated with the teleseismic waves are sufficient to start the 3-week-long failure process that is an ETS event. Admittedly, the small sample size (9 ETS events) may not be statistically significant, but provides hints of a causal relationship worthy of reporting.

9. Summary and Conclusions

[45] We have elucidated some of the physical conditions and processes necessary for triggering of tremor by examining seismic and other data during and immediately after the arrival of seismic waves from 30 teleseismic and 17 regional/local earthquakes on Vancouver Island, British Columbia. These earthquakes produced the strongest shaking to strike Vancouver Island during 1996–2007. We identify tremor triggered by four teleseismic earthquakes and note that tremor cannot be distinguished from energy radiated from posited triggering regional/local earthquakes, leaving open the possibility that these and even smaller, more frequent local events may commonly trigger tremor.

[46] We find that the amplitude of the triggering waves influences the likelihood of tremor triggering, but local conditions also are important. As was the case for the Oaxaca earthquake, triggered tremor appears more likely to occur in close proximity to ambient tremor and aseismic slip (in both space and time). This suggests that slow slip and/or high tremor rates indicate a regions closeness to failure and that triggered tremor is more likely to occur in the presence of ongoing tremor and slow slip.

[47] Our results also indicate that the local frictional properties control tremor and earthquake triggering. As has been suggested in studies of ambient tremor, if tremor and earthquakes represent different frictional regimes [*Yoshida and Kato*, 2003; *Liu and Rice*, 2005, 2007], one would expect triggered tremor and earthquakes to occur in different places. Our observations support this expectation.

Although the extraordinarily large amplitude 2002 Denali, Alaska earthquake waves triggered both tremor and earthquakes, their source locations are distinctly different. We note only ambiguous seismicity rate increases after a few other teleseisms, none of which correspond to the teleseisms that clearly triggered tremor. Ambient seismicity is sparse in the regions surrounding the tremor sources triggered by the Oaxaca and Volcano Islands earthquakes. The observations that may be contrary to this expectation are the locations of the tremor sources that were triggered by the Sumatra and Denali earthquake waves in an area of high ambient seismicity rates (Figure 1). However, we cannot rule out the possibility that they may be at differing depths given the uncertainties in the depth estimates of both the tremor and seismicity.

[48] We also note an interesting correlation between large teleseismic events and ETS episodes in the southern Vancouver Island/northern Puget Sound region. All the ETS events that have long interevent times also have a large teleseismic event that precedes them by several days. This suggests that for ETS events that are “late” and have built up more stress than usual, the slight nudge of the shaking from a large distant event may trigger the ETS episode.

[49] Our observations of tremor, earthquakes, and ETS all being triggered by earthquake waves indicate that their source faults respond to very small stresses (tens of kPa). Similarly, the small stresses associated with the Earth and ocean tides (~ 10 kPa) have been shown to influence the amplitude of ongoing tremor during ETS episodes [*Rubinstein et al.*, 2008]. All of this evidence suggests that tremor and earthquakes both occur on fault systems that are very close to failure because the induced shear stresses from the triggering events are much smaller than the expected lithostatic loads. The presence of high pore fluid pressure is one way in which these faults may be weakened, such that they can be influenced by the relatively small dynamic stresses from earthquakes and from tides.

Appendix A

[50] This and other studies of triggered tremor and earthquakes have made inferences about the causative deformation based on the phase relationship of the triggering and triggered signals [*Gomberg et al.*, 2008; *Miyazawa and Brodsky*, 2008; *Miyazawa and Mori*, 2005, 2006; *Peng et al.*, 2008; *Rubinstein et al.*, 2007; *Hill*, 2008; *Ghosh et al.*, submitted manuscript, 2008; *Peng et al.*, submitted manuscript, 2008]. Both tremor [*Miyazawa and Brodsky*, 2008; *Miyazawa and Mori*, 2005, 2006] and earthquakes [*West et al.*, 2005] appear to correlate with dilatational stresses or strains. This requires correcting for the difference in the observation and source locations, since the former are at the surface and the latter are typically elsewhere kilometers beneath the surface. Several studies have extrapolated to depth assuming an analytic solution of Raleigh wave propagation in a homogenous half-space. In this section we examine this extrapolation more generally, and show that while a correlation between the phasing of surface ground motions and dilatational stresses or strains at depth implies a correlation at depth, inferences about whether they are compressional or extensional may be uncertain.

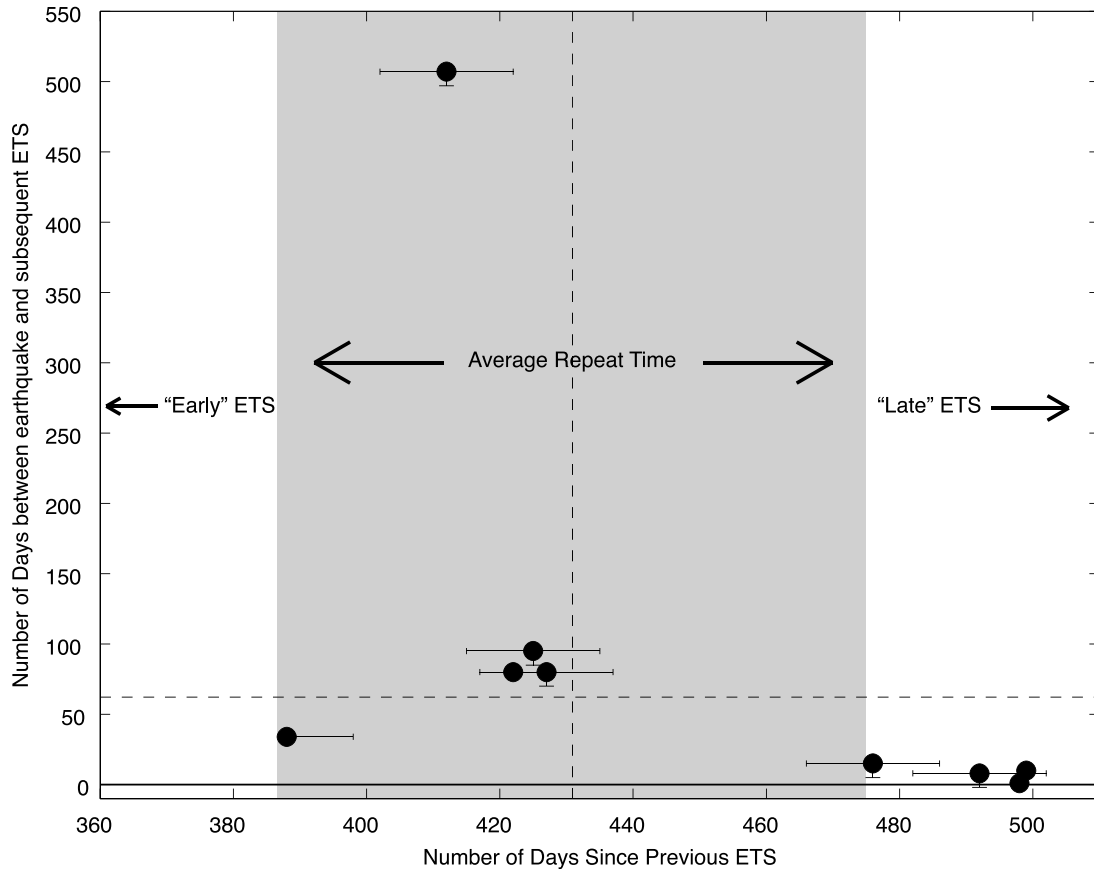


Figure 11. Temporal relationship between the 30 teleseismic earthquakes we considered and documented ETS episodes on Vancouver Island. Each dot represents an individual ETS episode with the horizontal axis showing the time between the ETS episode onset and the previous one. The number of days between the most recent teleseismic earthquake and the ETS episode is plotted on the vertical axis. Typically, there are multiple teleseismic earthquakes between the two ETS events, and we are examining the one closest to the start of the more recent ETS event. The horizontal dashed line shows the median number of days that we would expect that an ETS would be preceded by one of the 30 earthquakes if that ETS occurred on a randomly chosen day. The shaded region represents one standard deviation from the average ETS repeat time. ETS episodes to the right or left of this shaded region could be considered late or early, respectively. The onset times of ETS episodes are based on tremor observations analyzed by Rogers [2007], supplemented with information from the Pacific Northwest Seismic Network tremor Web sites, e.g., <http://www.pnsn.org/WEBICORDER/DEEPTREM/winter2008.html>. ETS episodes with uncertain start dates (1995–2002) have nominal error bars of 10 days, which is the time between the first observations of tremor in the United States and in Canada for the 2007 ETS episode. For those points where we have both Canadian and American data (2003–2007), we assign zero error. Vertical error bars only go down because the ETS events started no later than the first observations of tremor reported. The ETS event in the bottom left has a one sided error bar because its start time in 2003 is confidently known, but those of its predecessor are not so that the lapse time between the events might be longer than predicted, but not shorter. No large teleseisms in our set occurred between the 1998 and 1999 ETS events, giving rise to the largest interval between preceding teleseism and ETS event at >500 days.

[51] We examine the phase relation between Rayleigh waves at the surface and at depth in the frequency domain, describing the radial displacement, u_r , and vertical displacement, u_z , of a single mode of a Rayleigh wave as

$$u_r = R(\omega, z) \sin(kr - \omega t) \quad (\text{A1a})$$

$$u_z = Z(\omega, z) \cos(kr - \omega t) \quad (\text{A1b})$$

$R(\omega, z)$ and $Z(\omega, z)$ describe the radial and vertical displacement solutions, respectively, that solve the equation of

motion and boundary conditions that give rise to modal surface waves in a laterally homogeneous layered medium. ω denotes frequency, z denotes depth, t denotes time, r denotes horizontal distance, and k is the wave number. Positive z corresponds to upward motion from the surface. The dilatational strain equals

$$\Delta = \frac{du_r}{dr} + \frac{du_z}{dz} \quad (\text{A2})$$

The Love wave (tangential) displacement derivative, $du_\phi/d\phi$, equals zero because a Love wave is a horizontally

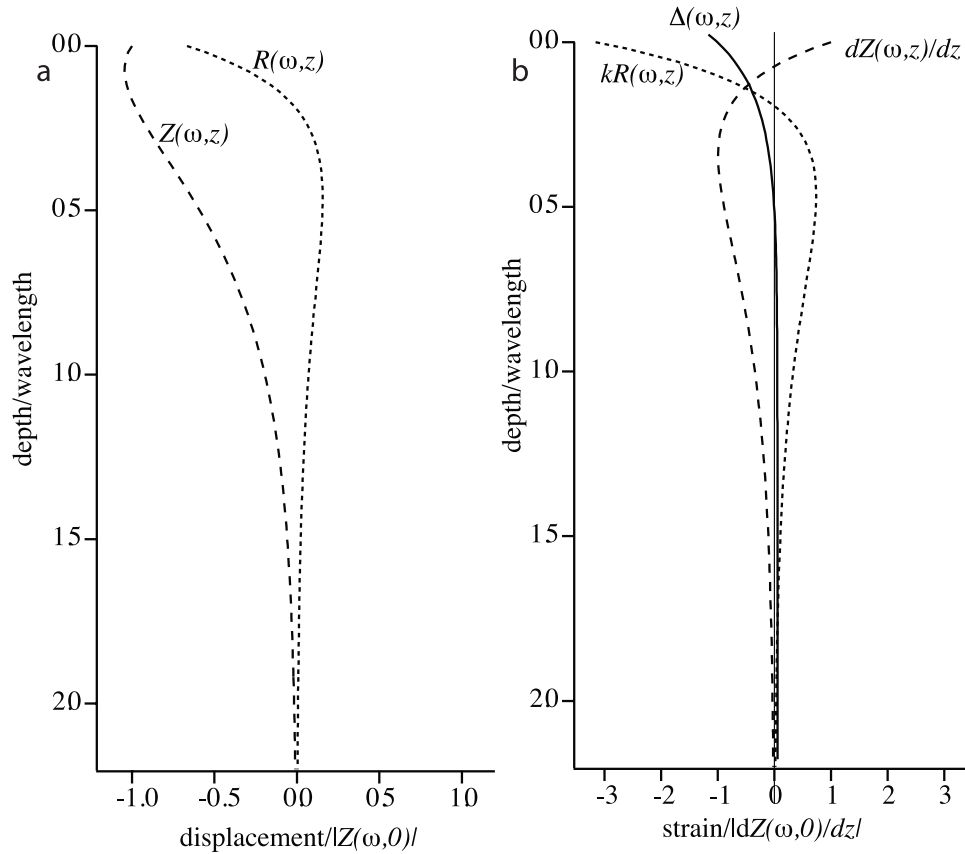


Figure A1. Functions describing the amplitude and signs of Rayleigh wave displacements and strains calculated for a homogeneous half-space, with shear, compressional, and Rayleigh wave velocities equal to 3.8, 6.5, and 3.5 km/s. These depend on frequency, ω , and depth, z (see text). (a) Radial and vertical displacements, $R(\omega, z)$ and $Z(\omega, z)$, respectively, normalized by the latter at the surface. (b) The radial and vertical displacement gradients are proportional to $kR(\omega, z)$ and $dZ(\omega, z)/dz$ and the dilatational strain, $\Delta(\omega, z)$, to their sum.

traveling plane wave in which the wavefront is aligned along the tangential direction. Expansive strains are positive and the stress is proportional to Δ with the bulk modulus defining the constant of proportionality, such that compressive stresses are negative.

[52] To see the connection between Δ and the displacement field, we taking the time derivative of u_r (equation A1b),

$$\frac{du_r}{dt} = -\omega R(\omega, z) \cos(kr - \omega t) \quad (\text{A3})$$

and substitute it and equation (A1a) into equation (A2), yielding

$$\Delta = \left[kR(\omega, z) + \frac{dZ(\omega, z)}{dz} \right] \cos(\omega t - kr) \quad (\text{A4})$$

Thus, noting that $k = \omega/C_R$ with $C_R(\omega)$ equal to the Rayleigh wave phase velocity, the dilatational strain can be written as

$$\begin{aligned} \Delta &= -C_R^{-1}(\omega) \frac{du_r}{dt} + \frac{1}{Z(\omega, z)} \frac{dZ(\omega, z)}{dz} u_z \\ &= -C_R^{-1}(\omega) \frac{du_r}{dt} + \frac{d \ln Z(\omega, z)}{dz} u_z \end{aligned} \quad (\text{A5})$$

[53] We now have the descriptions needed to examine the phase relationship between the radial and vertical component displacements and velocities observed at the surface and the dilatational stresses at depth. Equations (A1) and (A5) show that the dilatation will differ in phase by 0° or 180° relative to the vertical displacement, u_z , and the radial velocity, du_r/dt . Resolving these 180° ambiguities depends on the relative sizes and signs of $dZ(\omega, z)/dz$, $Z(\omega, z)$, and $kR(\omega, z)$. These and their variation with depth depend on the rheologic stratification of the Earth structure and the frequency of the Rayleigh wave. This is evident from the analytic expressions for Rayleigh wave motions and deformations in a homogeneous half-space, which show that the signs and magnitudes of both $R(\omega, z)$ and $dZ(\omega, z)/dz$ change with depth (Figure A1). Numerical computations of $R(\omega, z)$ and $Z(\omega, z)$ for a standard stratified Gutenberg Earth model show the same general characteristics, although the details differ [see *Aki and Richards*, 1980, Box 7.5].

[54] As other studies have shown, for the homogeneous half-space model, although the terms in equations (A4) and (A5) vary in size and sign with depth, both the dilatational strain and vertical displacement remain in phase at all depths. The radial velocity changes sign however, at ~ 0.2 of a wavelength, or at 14 to 32 km (corresponding to periods of 20–40 s). This is close enough to the depth

range at which most triggering earthquakes and tremor occur to make inferences from surface observations of radial motions about dilatational or compressive stresses at source depths ambiguous. Moreover, while equation (A5) does show that Δ should be in phase or 180° out of phase with du_r/dt and u_z , at all depths, it isn't clear that this ambiguity can be resolved for more general Earth models. In other words, the phasing between triggering waves and triggered earthquakes or tremor observed at the surface may be used to infer a correlation (or lack of) with dilatational stresses at source depths, but inferences about whether they are compressional or extensional are uncertain. Exploration of the generality of the behavior of the homogeneous half-space model predictions for more realistic Earth structures should be undertaken in future studies.

[55] **Acknowledgments.** We thank Tim Melbourne for his assistance with GPS data and helpful conversations. Conversations with Emily Brodsky, Herb Dragert, Heidi Houston, and Masatoshi Miyazawa provided useful insight and improved this manuscript. Reviews by David Shelly, Paul Spudich, and two anonymous reviewers significantly improved this manuscript. The seismic data from Vancouver Island comes from the Canadian National Seismograph Network and are distributed freely by The Geological Survey of Canada. The Pacific Northwest Seismic Network provided the seismic data from Washington.

References

- Aki, K., and P. G. Richards (1980), *Quantitative Seismology, Theory and Methods*, vol. 1, W.H. Freeman, San Francisco, Calif.
- Beeler, N. M., and D. A. Lockner (2003), Why earthquakes correlate weakly with the solid Earth tides: Effects of periodic probability of earthquake occurrence, *J. Geophys. Res.*, *108*(B8), 2391, doi:10.1029/2001JB001518.
- Braunmiller, J., and J. Na'bilek (2002), Seismotectonics of the Explorer region, *J. Geophys. Res.*, *107*(B10), 2208, doi:10.1029/2001JB000220.
- Brodsky, E. E., and S. G. Prejean (2005), New constraints on mechanisms of remotely triggered seismicity at Long Valley Caldera, *J. Geophys. Res.*, *110*, B04302, doi:10.1029/2004JB003211.
- Cassidy, J. F., R. M. Ellis, C. Karavas, and G. C. Rogers (1998), The northern limit of the subducted Juan de Fuca plate system, *J. Geophys. Res.*, *103*, 26,949–26,961, doi:10.1029/98JB02140.
- Cassidy, J. F., G. C. Rogers, and F. Waldhauser (2000), Characterization of active faulting beneath the Strait of Georgia, British Columbia, *Bull. Seismol. Soc. Am.*, *90*, 1188–1199, doi:10.1785/0120000044.
- Daniel, G., D. Marsan, and M. Bouchon (2008), Earthquake triggering in southern Iceland following the June 2000, M_w 6.6 doublet, *J. Geophys. Res.*, *113*, B05310, doi:10.1029/2007JB005107.
- Gomberg, J., and P. Johnson (2005), Seismology: Dynamic triggering of earthquakes, *Nature*, *437*, 830, doi:10.1038/437830a.
- Gomberg, J., K. Shedlock, and S. Roecker (1990), The effect of S wave arrival times on the accuracy of hypocenter estimation, *Bull. Seismol. Soc. Am.*, *80*, 1605–1628.
- Gomberg, J., M. Blanpied, and N. M. Beeler (1997), Transient triggering of near and distant earthquakes, *Bull. Seismol. Soc. Am.*, *87*, 294–309.
- Gomberg, J., J. L. Rubinstein, Z. Peng, K. C. Creager, J. E. Vidale, and P. Bodin (2008), Widespread triggering of nonvolcanic tremor in California, *Science*, *319*, 173, doi:10.1126/science.1149164.
- Hill, D. P. (2008), Dynamic stresses, Coulomb failure, and remote triggering, *Bull. Seismol. Soc. Am.*, *98*, 66–92, doi:10.1785/0120070049.
- Hill, D. P., and S. G. Prejean (2007), Dynamic triggering, in *Earthquake Seismology*, vol. 4, *Treatise on Geophysics*, edited by H. Kanamori, chap. 8, pp. 257–291, Elsevier, Amsterdam.
- Ide, S., D. R. Shelly, and G. C. Beroza (2007), Mechanism of deep low frequency earthquakes: Further evidence that deep nonvolcanic tremor is generated by shear slip on the plate interface, *Geophys. Res. Lett.*, *34*, L03308, doi:10.1029/2006GL028890.
- Johnson, P., and X. Jia (2005), Nonlinear dynamics, granular media and dynamic earthquake triggering, *Nature*, *437*, 871–874, doi:10.1038/nature04015.
- Kao, H., S. Shan, H. Dragert, G. Rogers, J. F. Cassidy, and K. Ramachandran (2005), A wide depth distribution of seismic tremors along the northern Cascadia margin, *Nature*, *436*, 841–844, doi:10.1038/nature03903.
- Kao, H., S.-J. Shan, H. Dragert, G. Rogers, J. F. Cassidy, K. Wang, T. S. James, and K. Ramachandran (2006), Spatial-temporal patterns of seismic tremors in northern Cascadia, *J. Geophys. Res.*, *111*, B03309, doi:10.1029/2005JB003727.
- Kao, H., S.-J. Shan, G. Rogers, and H. Dragert (2007a), Migration characteristics of seismic tremors in the northern Cascadia margin, *Geophys. Res. Lett.*, *34*, L03304, doi:10.1029/2006GL028430.
- Kao, H., P. J. Thompson, G. Rogers, H. Dragert, and G. Spence (2007b), Automatic detection and characterization of seismic tremors in northern Cascadia, *Geophys. Res. Lett.*, *34*, L16313, doi:10.1029/2007GL030822.
- Lewis, T. J., C. Lowe, and T. S. Hamilton (1997), Continental signature of a ridge-trench-triple junction: Northern Vancouver Island, *J. Geophys. Res.*, *102*, 7767–7781.
- Liu, Y., and J. R. Rice (2005), Aseismic slip transients emerge spontaneously in three-dimensional rate and state modeling of subduction earthquake sequences, *J. Geophys. Res.*, *110*, B08307, doi:10.1029/2004JB003424.
- Liu, Y., and J. R. Rice (2007), Spontaneous and triggered aseismic deformation transients in a subduction fault model, *J. Geophys. Res.*, *112*, B09404, doi:10.1029/2007JB004930.
- McCroly, P. A., J. L. Blair, D. H. Oppenheimer, and S. R. Walter (2003), Depth to the Juan de Fuca slab beneath the Cascadia subduction margin: A 3-D model for sorting earthquakes [CD-ROM], *U. S. Geol. Surv. Digital Data Ser.*, *91*, 13 pp.
- Miyazawa, M., and E. E. Brodsky (2008), Deep low-frequency tremor that correlates with passing surface waves, *J. Geophys. Res.*, *113*, B01307, doi:10.1029/2006JB004890.
- Miyazawa, M., and J. Mori (2005), Detection of triggered deep low-frequency events from the 2003 Tokachi-oki earthquake, *Geophys. Res. Lett.*, *32*, L10307, doi:10.1029/2005GL022539.
- Miyazawa, M., and J. Mori (2006), Evidence suggesting fluid flow beneath Japan due to periodic seismic triggering from the 2004 Sumatra-Andaman earthquake, *Geophys. Res. Lett.*, *33*, L05303, doi:10.1029/2005GL025087.
- Miyazawa, M., E. E. Brodsky, and J. Mori (2008), Learning from dynamic triggering of low-frequency tremor in subduction zones, *Earth Planets Space*, *60*, e17–e20.
- Nadeau, R., and D. Dolenc (2005), Nonvolcanic tremors deep beneath the San Andreas fault, *Science*, *307*, 389, doi:10.1126/science.1107142.
- Obara, K. (2002), Nonvolcanic deep tremor associated with subduction in southwest Japan, *Science*, *296*, 1679–1681, doi:10.1126/science.1070378.
- Peacock, S. M., K. Wang, and A. M. McMahon (2002), Thermal structure and metamorphism of subducting oceanic crust: Insight into Cascadia intraslab earthquakes, in *The Cascadia Subduction Zone and Related Subduction Systems: Seismic Structure, Intraslab Earthquakes and Processes, and Earthquake Hazards*, edited by S. Kirby et al., *U. S. Geol. Surv. Open File Rep.*, *02–328*, pp. 123–126.
- Peng, Z., and K. Chao (2008), Non-volcanic tremors underneath the Central Range in Taiwan triggered by the 2001 M_w 7.8 Kunlun earthquake, *Geophys. J. Int.*, *175*, 825–829, doi:10.1111/j.1365-246X.2008.03886.x.
- Peng, Z., J. E. Vidale, K. C. Creager, J. L. Rubinstein, J. Gomberg, and P. Bodin (2008), Strong tremor near Parkfield, CA, excited by the 2002 Denali Fault earthquake, *Geophys. Res. Lett.*, *35*, L23305, doi:10.1029/2008GL036080.
- Ristau, J., G. C. Rogers, and J. F. Cassidy (2007), Stress in western Canada from regional moment tensor analysis, *Can. J. Earth Sci.*, *44*, 127–148, doi:10.1139/E06-057.
- Rogers, G. (2007), Episodic tremor and slip in northern Cascadia: Going back in time, paper presented at Seismological Society of America Annual Meeting, Waikoloa, Hawaii, 11–13 April.
- Rogers, G., and H. Dragert (2003), Episodic tremor and slip on the Cascadia subduction zone: The chatter of silent slip, *Science*, *300*, 1942–1943, doi:10.1126/science.1084783.
- Rubinstein, J. L., J. E. Vidale, J. Gomberg, P. Bodin, K. C. Creager, and S. D. Malone (2007), Non-volcanic tremor driven by large transient shear stresses, *Nature*, *448*, 579–582, doi:10.1038/nature06017.
- Rubinstein, J. L., M. LaRocca, J. E. Vidale, K. C. Creager, and A. G. Wech (2008), Tidal modulation of nonvolcanic tremor, *Science*, *319*, 186–189, doi:10.1126/science.1150558.
- Savage, H. M., and C. Marone (2007), Effects of shear velocity oscillations on stick-slip behavior in laboratory experiments, *J. Geophys. Res.*, *112*, B02301, doi:10.1029/2005JB004238.
- Shelly, D. R., G. C. Beroza, S. Ide, and S. Nakamura (2006), Low-frequency earthquakes in Shikoku, Japan, and their relationship to episodic tremor and slip, *Nature*, *442*, 188–191, doi:10.1038/nature04931.
- Szeliga, W., T. I. Melbourne, V. M. Santillan, and M. M. Miller (2008), GPS constraints on 34 slow slip events within the Cascadia subduction zone, 1997–2005, *J. Geophys. Res.*, *113*, B04404, doi:10.1029/2007JB004948.

- Toda, S., R. S. Stein, K. Richards-Dinger, and S. B. Bozkurt (2005), Forecasting the evolution of seismicity in southern California: Animations built on earthquake stress transfer, *J. Geophys. Res.*, *110*, B05S16, doi:10.1029/2004JB003415.
- Voisin, C., F. Cotton, and S. Di Carli (2004), A unified model for dynamic and static stress triggering of aftershocks, antishocks, remote seismicity, creep events, and multisegmented rupture, *J. Geophys. Res.*, *109*, B06304, doi:10.1029/2003JB002886.
- Wech, A. G., and K. C. Creager (2007), Cascadia tremor polarization evidence for plate interface slip, *Geophys. Res. Lett.*, *34*, L22306, doi:10.1029/2007GL031167.
- West, M., J. J. Sanchez, and S. R. McNutt (2005), Periodically triggered seismicity at Mount Wrangell, Alaska, after the Sumatra earthquake, *Science*, *308*, 1144–1146, doi:10.1126/science.1112462.
- Yoshida, S., and N. Kato (2003), Episodic aseismic slip in a two-degree-of-freedom block-spring model, *Geophys. Res. Lett.*, *30*(13), 1681, doi:10.1029/2003GL017439.
-
- K. C. Creager, J. E. Vidale, and A. G. Wech, Department of Earth and Space Science, University of Washington, P.O. Box 351310, Seattle, WA 98195, USA.
- J. Gomberg, U.S. Geological Survey, University of Washington, P.O. Box 351310, Seattle, WA 98195, USA.
- H. Kao and G. Rogers, Geological Survey of Canada, 9860 West Saanich Road, Sidney, BC V8L 4B2, Canada.
- J. L. Rubinstein, U.S. Geological Survey, 345 Middlefield Road, MS-977, Menlo Park, CA 94025, USA. (jl.rubinstein@usgs.gov)